Scilight

Nano-electrochemistry & Nano-photochemistry

https://www.sciltp.com/journals/nenp

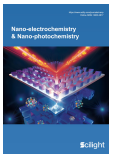

Review

Supercapacitors in Bioelectronics: Materials, Biocompatibility, and *In Vivo* Applications

Yanlin Li, Jie Ji, Changdao Han, Tao Liu * and Limin Zhang *

Department School of Chemistry and Molecular Engineering, East China Normal University, Shanghai 200241, China
* Correspondence: taoliu@chem.ecnu.edu.cn (T.L.); lmzhang@chem.ecnu.edu.cn (L.Z.)

How To Cite: Li, Y.; Ji, J.; Han, C.; et al. Supercapacitors in Bioelectronics: Materials, Biocompatibility, and *In Vivo* Applications. *Nano-electrochemistry & Nano-photochemistry* **2026**, *2*(2), 10. https://doi.org/10.53941/nenp.2026.100010

Received: 6 March 2026
Revised: 6 May 2026
Accepted: 8 May 2026
Published: 19 May 2026

Abstract: Supercapacitors are increasingly being explored for bioelectronic systems due to their high power density, rapid charge–discharge capability, and excellent biocompatibility, making them promising for tissue–device interfaces. This review summarizes recent advances in supercapacitor materials and device architectures, with particular emphasis on their electrochemical performance, biocompatibility, and multifunctionality in biological applications. To meet diverse application requirements, various one-dimensional fibers, two-dimensional planar structures, and three-dimensional materials have been developed. These supercapacitors can also be integrated with bioelectronic devices such as biofuel cells, enabling combined bioelectrochemical energy conversion and capacitive energy storage. Importantly, many supercapacitors designed for biomedical use exhibit excellent biocompatibility, and some are even biodegradable, thereby providing a solid foundation for *in vivo* applications. In addition, supercapacitor-based platforms have been engineered to simultaneously deliver energy and provide electrical stimulation to cells, tissues, and *in vivo* environments. Consequently, supercapacitor-driven bioelectronics are steadily advancing toward wearable and implantable biomedical devices.

Keywords: supercapacitors; materials and structures; biocompatibility; degradability; *in vivo* applications

1. Introduction

In recent years, continuous breakthroughs in materials science, information technology, and advanced manufacturing have accelerated the development of electronic devices across a wide range of applications, including healthcare, security, and environmental monitoring [1–3]. Bioelectronics is a particularly promising field with significant growth potential. It has been widely explored for drug delivery, biosensing, and biological modulation, and shows considerable therapeutic value in treating diverse diseases and disorders, such as Parkinson's disease, congenital heart defects, and paralysis [4–7]. Supercapacitors have emerged as attractive energy-storage units for bioelectronic systems [8,9]. Compared with batteries and conventional capacitors, supercapacitors offer high specific capacitance and power density [10–12], improved mechanical compliance for tissue integration, and generally favorable biocompatibility [13–16]. Nevertheless, the charge-storage mechanism of supercapacitors intrinsically limits their energy density, which remains considerably lower than that of batteries [17–19]. Therefore, extensive efforts have focused on enhancing their energy density. Effective strategies include developing porous and nanoscale electrode materials to increase capacitance and constructing hybrid or asymmetric supercapacitors to expand the operating voltage window and improve overall energy output [20].

As bioelectronic devices are increasingly deployed for *in vivo* analysis [21,22], concerns regarding biocompatibility and long-term safety have become more prominent [23,24]. Traditional macroscale bioelectronic devices are often rigid and exhibit pronounced mechanical mismatch with soft, dynamic tissues [25–27]. This

mismatch limits conformal contact, intensifies micromotion at the tissue–device interface, and promotes local irritation and tissue injury [28–30]. During chronic implantation, it can trigger inflammation and fibrotic encapsulation, thereby compromising long-term reliability and safety [31–34]. Biocompatibility is therefore a primary requirement for biointerfacing electronics, encompassing mechanical compliance, chemical safety, and interfacial stability [35–37]. In addition, practical applications often involve repeated deformation or accidental mechanical damage, which can cause performance degradation. Thus, it is crucial to develop supercapacitor materials and devices with high stretchability and, ideally, self-healing capability [38–41]. Flexible supercapacitors provide an attractive energy-storage option for biomedical systems [42–44]. Flexible electrodes improve mechanical compliance, and biocompatible electrolytes reduce leakage and toxicity risk. Ion-rich gels and hydrogels are common choices. Soft encapsulation layers protect tissues and stabilize interfaces. Flexible supercapacitors tolerate repeated deformation, maintain electrochemical performance under bending and stretching, and deliver high power for pulsed operation, supporting stable sensing and stimulation [45,46]. Depending on the level of biointerface interaction, such devices can be implemented in skin-contact and skin-adhering formats for continuous physiological monitoring.

Beyond long-term biocompatibility, some implantable scenarios require devices to disappear after completing their tasks to avoid secondary surgical retrieval and associated risks [47–50]. Implantable medical electronic devices (IEMDs) have been increasingly adopted to address the growing burden of neurological and cardiovascular diseases [51–54]. Typical examples include implantable biosensors, pacemakers, defibrillators, and stimulators for deep-brain, bone, and peripheral-nerve applications [55–57]. Long-term *in vivo* diagnosis and therapy impose stringent requirements on IEMDs, including high biocompatibility, miniaturization, and operational stability. Most IEMDs are currently powered by non-degradable batteries. Such power sources often necessitate surgical retrieval after the intended function is completed, introducing additional risk and patient burden [58,59]. To reduce these limitations, increasing attention has shifted to transient electronic energy-storage systems [60,61]. These devices are designed to degrade after use, with by-products that can be safely resorbed or cleared by the body. This strategy has been extended to biomedical uses, including controlled drug-release platforms and temporary sensors deployed in organs such as the brain and heart [62,63]. Degradable supercapacitors have therefore attracted interest as implantable power supplies [64,65]. A variety of bioresorbable or biofluid-degradable materials have been explored as electrodes, electrolytes, and encapsulation layers. Encapsulation design enables programmable dissolution, allowing devices to fully or partially degrade in physiological media. As a result, supercapacitors can function as transient energy-storage units for IEMDs and provide an effective route to controlling device lifetime and *in vivo* operating duration.

Supercapacitors can also be directly utilized for electrical stimulation of nerves and tissues, extending their role beyond energy storage in bioelectronic systems. A representative study reported a device that integrates a multiscale porous material architecture with an interdigitated microelectrode layout, delivering supercapacitor-like electrochemical performance [66]. The device enabled modulation of cardiomyocytes (CMs) in vitro, excitation of isolated hearts and retinal tissues ex vivo, and stimulation of sciatic nerves *in vivo* under physiologically relevant conditions. These advances highlight the practical potential of supercapacitor-inspired platforms for bioelectric therapeutics, while also underscoring the importance of material selection, biocompatibility, and mechanically compliant designs for reliable *in vivo* operation.

2. Materials and Device Designs

2.1. Materials and Structures of Supercapacitors

To date, supercapacitors are generally designed based on two fundamental charge-storage mechanisms: electric double-layer capacitance (EDLC) and pseudocapacitance [67–69]. EDLCs store energy via the non-Faradaic adsorption of electrostatic charges at the electrode–electrolyte interface. Accordingly, EDLC electrodes are expected to provide a large accessible surface area, high electronic conductivity, and a sufficiently wide and stable operating potential window. Carbon-based materials meet these requirements well because of their high specific surface area, good electrical conductivity, and excellent chemical stability. A wide range of carbon materials–including activated carbon, carbon nanotubes (CNTs), porous carbon, and graphene–has therefore been extensively investigated as EDLC electrodes in recent years [70–73].

In contrast to the interfacial charge adsorption in EDLCs, pseudocapacitors rely on fast and reversible faradaic redox reactions occurring on or near the surface of electroactive materials, enabling higher capacitance and energy storage through charge-transfer processes [74–76]. This mechanism places additional demands on electrode materials, including abundant redox-active sites, rapid ion/electron transport for high-rate charge–discharge, and adequate electrical conductivity. Typical pseudocapacitive materials include transition-metal

oxides/hydroxides and conductive polymers. Among them, Ni- and Co-based oxides, as well as related hydroxides, have attracted considerable attention as pseudocapacitive electrodes due to their favorable electronic transport properties and rich redox chemistry [77–79]. Conducting polymers such as polyacetylene (PA), polypyrrole (PPy), polyaniline (PANI), and poly(3,4-ethylenedioxythiophene) (PEDOT) are also regarded as promising candidates, benefiting from their intrinsic conductivity and tunable redox behavior [80–84].

Driven by the increasing demand for higher energy density and broader application scenarios, a growing number of emerging material families have been introduced into supercapacitor research [85], including MXenes [86,87], metal–organic frameworks (MOFs) [88,89], polyoxometalates (POMs) [90], and black phosphorus (BP) [91,92]. These materials not only expand the available material toolbox but may also enable new charge-storage pathways through tailored structures and surface chemistries. Beyond material innovation, structural engineering provides another effective lever to optimize device performance and functionality. Both EDLCs and pseudocapacitors can be constructed into one-dimensional (1D) fiber, two-dimensional (2D) planar, or three-dimensional (3D) architectures, thereby accommodating diverse requirements such as flexibility, integration density, and application-specific form factors.

2.1.1. 1D Fiber Supercapacitors

Fiber supercapacitors offer excellent flexibility and strong potential for implantable applications [93–95]. Fiber-shaped devices can be introduced into blood vessels, and fibrous structures are inherently compatible with surgical suturing for wound closure. Their slender geometry also occupies minimal space *in vivo*, thereby reducing constraints on natural motion.

Researchers presented a thermal drawing process (TDP) to manufacture tough hydrogel-based biocompatible supercapacitor (THBS) fibers specially designed for safe, long-term *in vivo* implantation (Figure 1(Ai)) [96]. This approach enables mass production by scaling down a preform from the centimeter to micrometer dimensions, achieving a highly adaptable form factor (bending stiffness of the THBS fibers ~10.3 N/m). With a thickness of only a few hundred microns, these highly flexible THBS fibers allow minimally invasive insertion and adaptable placement throughout various tissues and organs. The fiber achieved a maximum areal capacitance of 268 mF/cm^2 and volumetric capacitance of 18.8 F/cm^3. The THBS fiber retained 96.48% of its initial capacitance after 1000 cycles of 90° bending.

Qu et al. present an integrated fiber device consisting of a shape-adjustable, packable, and energy-controllable wireless charging coil and supercapacitor (WC-SC) (Figure 1(Aii)) [97]. The integrated device, which combines wireless charging and energy storage functions, is fabricated entirely from flexible carbon fibers (CFs). The resulting WC-SC can undergo large shape deformations, with its diameter varying from 2 cm to 20 cm. Owing to its ultrahigh flexibility, the device can be packed into various irregular spaces, such as a smart bracelet, a disk-shaped pet GPS, and other wearable electronics. Meanwhile, the harvested energy of the wireless charging coil can be readily tuned by altering the shape of the WC-SC. In addition, the integrated supercapacitor in the WC-SC exhibits an areal capacitance of 803 mF cm^{-2} and an energy density of 1004 μWh cm^{-2}, which are higher than those of most reported fiber supercapacitors. This fiber-based packable WC-SC, with its controllable shape, size, and energy output, shows strong potential for integration into a wide range of practical applications.

Other stretchable architectures have also been proposed. Helical or spring-like structures can be formed by winding fiber electrodes around a stretchable substrate or electrolyte, thereby accommodating large strain. Reduced graphene oxide (RGO) fiber-based springs have been used as electrodes for stretchable and self-healing supercapacitors. Graphene fibers are attractive electrode materials due to their high electrical and thermal conductivity, elasticity, and chemical stability. However, conventional graphene-based fiber electrodes are often thin and vulnerable to mechanical damage, which can compromise the performance and reliability of supercapacitors. To overcome this limitation, a spring-like RGO-based composite fiber capable of stretching to 300% was reported [98]. A self-healing, stretchable carboxylated polyurethane (PU) coating was applied to the spring-like electrodes. This coating guided reconnection of fractured spring segments, enabling self-healing and partial recovery of electrical properties. The supercapacitor maintained 82.4% capacitance retention under 100% stretching and remained at 54.2% after the third healing cycle.

Many of the strategies discussed above rely on embedding relatively rigid miniature devices into elastomeric substrates. By comparison, microscale elastic conductive fibers that can sustain large reversible strains offer distinct advantages for electronic systems requiring high tensile deformability. As shown in Figure 1(Aiii), Ray H. Baughman and co-workers fabricated superelastic conductive fibers by wrapping multilayer multiwalled carbon nanotube sheets (NTSs) around pre-stretched rubber fibers, followed by sequential release, re-stretching, and release [99]. This process produced a hierarchical buckled NTS sheath–core structure that could be reversibly

elongated to more than ten times its initial length, while limiting the resistance change to ~5%. Dai and co-workers developed a wire-shaped supercapacitor with an elastic strain exceeding 350% by twisting two elastic CNT-wrapped wires with a polymer electrolyte sandwiched between them [100]. The elastic threads were pre-coated with poly(vinyl alcohol)/H_3PO_4 hydrogel, which served as both electrolyte and separator. The resulting linear supercapacitor delivered a gravimetric capacitance as high as 30.7 F g^{-1}. This core–shell configuration provides a large ion-accessible surface area and a compact device footprint, contributing to improved electrochemical performance.

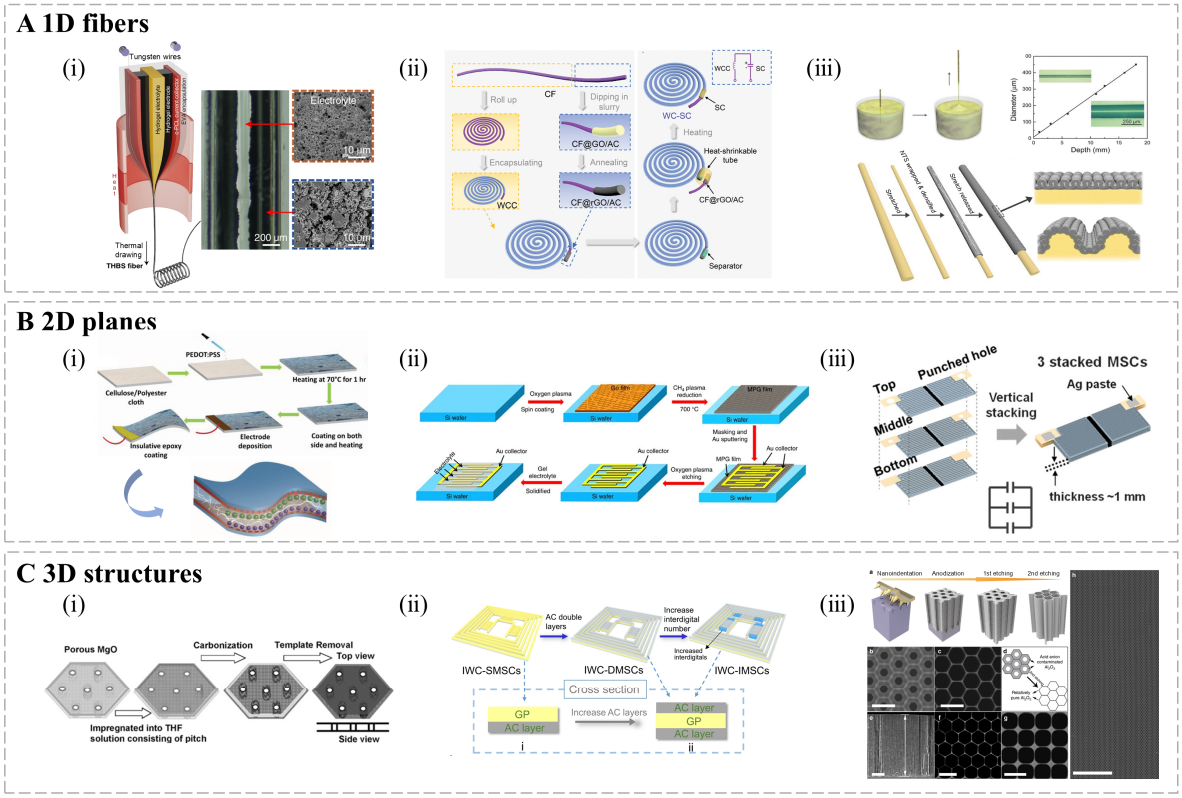

Figure 1. Three main structure designs for supercapacitors. (**A**) 1D fibers. (**i**) THBS fibers. The preform contains PVA-based hydrogel electrodes, PVA-based hydrogel electrolyte, c-PCL current collector, EVA encapsulation, and tungsten wires [96]. Copyright 2025 Springer Nature. (**ii**) Schematic illustration of the fabricating process for one electrode of the WCC part, SC part and the SC assembly process in WC-SC [97]. Copyright 2024 Wiley-VCH. (**iii**) Superelastic conductive fiber supercapacitor [99]. Copyright 2016 Wiley-VCH. (**B**) 2D planes. (**i**) Sandwich-type supercapacitor [101]. Copyright 2020 Wiley-VCH. (**ii**) Schematic illustration of the fabrication of MPG-MSCs [102]. Copyright 2013 Springer Nature. (**iii**) Planar all-solid-state MSC arrays [103]. Copyright 2016 American Chemical Society. (**C**) 3D structures. (**i**) 3D columnar porous carbon nanosheet (PPCN) supercapacitor [104] Copyright 2012 Wiley-VCH. (**ii**) Schematic diagrams of the procedure of optimizing MSCs in IWC-MSCs [105]. Copyright 2021 Springer Nature. (**iii**) Fabrication and structure of HAN [106]. Copyright 2020 Springer Nature.

2.1.2. 2D Planar Supercapacitors

Two-dimensional (2D) planar supercapacitors can be fabricated using sputtering [107], spin or spray coating [108], chemical vapor deposition (CVD) [109], and layer-by-layer assembly. Early studies were largely dominated by conventional sandwich-type configurations, which typically consist of two thin-film electrodes separated by a solid-state electrolyte layer that also functions as the separator.

Ravinder Dahiya and co-workers reported a sweat-based flexible supercapacitor for self-powered smart textiles and wearable systems using a simple, low-cost drop-casting process [101]. As shown in Figure 1(Bi), polyester–cellulose cloth served simultaneously as the substrate and separator, while PEDOT:PSS was deposited onto the cloth as both the electroactive material and current collector, forming a sandwich architecture. With human sweat as the electrolyte, the device delivered an energy density of 0.25 Wh kg^{-1} and a power density of 30.62 W kg^{-1}, demonstrating its potential as an on-body energy-storage unit for wearable electronics.

Although sandwich-type supercapacitors are straightforward to fabricate, their stacked architecture can hinder device miniaturization and system integration. Interdigitated electrodes offer a planar layout with short ion-transport pathways and a compact footprint, making them attractive for miniaturized energy-storage systems. Graphene-based

in-plane interdigital micro-supercapacitors were demonstrated on arbitrary substrates (Figure 1(Bii)) [102]. The resulting micro-supercapacitors deliver an area capacitance of 80.7 μF cm^{-2} and a volumetric capacitance of 17.9 F cm^{-3}. Furthermore, they exhibit a power density of 495 W cm^{-3}, which is higher than that of electrolytic capacitors, and an energy density of 2.5 mWh cm^{-3}, comparable to that of lithium thin-film batteries, together with superior cycling stability. These microdevices can operate at ultrahigh scan rates of up to 1,000 V s^{-1}, which is three orders of magnitude higher than that of conventional supercapacitors. Micro-supercapacitors with an in-plane geometry therefore show great promise for numerous miniaturized and flexible electronic applications.

The energy density of a single supercapacitor is generally limited. A simple and effective strategy to boost the overall energy output is to integrate multiple units into an array. An encapsulated, stretchable, high-performance stacked planar micro-supercapacitor (MSC) array has been reported [103]. As shown in Figure 1(Biii), a pair of planar all-solid-state MSCs was fabricated in tandem on a polyethylene terephthalate (PET) film, using spray-deposited multiwalled carbon nanotube (MWCNT) electrodes and drip-cast, UV-patternable ionic-gel electrolytes. For a single MSC, the operating voltage was 1.5 V. Connecting two MSCs in series doubled the output voltage. With the solid-state patterned electrolyte enabling reliable electrical isolation and interconnection, multiple MSCs could be vertically stacked and connected in parallel to increase the total and areal capacitance.

2.1.3. 3D Stereoscopic Supercapacitors

Compared with 1D and 2D configurations, three-dimensional (3D) architectures typically provide higher porosity and better mechanical compliance, enabling accommodation of multidirectional deformation [110,111]. Such stereoscopic structures establish continuous ion- and electron-transport pathways throughout the electrode framework, thereby improving electrolyte accessibility and promoting favorable electrochemical kinetics [112]. For 2D nanomaterials such as graphene, the high surface area and excellent electronic transport can be compromised by unavoidable sheet aggregation and restacking driven by interlayer van der Waals interactions [113,114]. This restacking reduces accessible surface area, blocks ion pathways, and degrades the effective utilization of individual layers. To mitigate these issues, a variety of approaches have been explored, including chemical/physical activation, fabrication of graphene nanonets, and insertion of nanocarbon spacers between nanosheets to suppress aggregation [115,116].

A template-assisted strategy for the scalable fabrication of 3D pillar-supported porous carbon nanosheet (PPCN) architectures was reported [104]. In this design, two carbon layers are fully separated and mechanically supported by carbon pillars (Figure 1(Ci)), forming an interconnected open-pore system and a self-supporting mesoporous conductive network. The PPCN structure provides high surface area and high overall conductivity, while simultaneously improving nanoscale ion transport by shortening diffusion distances and maintaining open channels. As a result, PPCN achieved a Brunauer–Emmett–Teller (BET) surface area of 883 m^2 g^{-1} and delivered a specific capacitance of 289 F g^{-1} at 2 mV s^{-1}, highlighting the electrochemical advantages enabled by the 3D architecture.

The researchers proposed a seamlessly integrated wireless charging micro-supercapacitor (IWC-MSC) by employing a designed highly consistent material system for both the wireless coils and the MSC electrodes (Figure 1(Cii)) [105]. The IWC-MSC device consists of three parallel MSC units, which are regarded as an integrated device for electrochemical measurements. The capacitance of the integrated MSC can be further enhanced by simply doubling the activated carbon (AC) electrode layers on both sides of the graphene paper (GP) substrate without introducing additional redundant devices. Accordingly, the structure of the integrated MSC device changes from a single-layer configuration to a double-layer architecture after incorporating extra AC electrodes on the opposite side of the GP substrate. The resulting device exhibits low internal resistance and excellent voltage tolerance, delivering a capacitance of 454.1 mF cm^{-2}. In addition, a record-high energy density of 463.1 μWh cm^{-2} surpasses those of existing metal-ion hybrid micro-supercapacitors and even commercial thin-film batteries (350 μWh cm^{-2}). After charging for 6 min, the integrated device can deliver a power output of up to 45.9 mW, which is sufficient to immediately drive an electric toy car.

Lei and co-workers reported microminiaturized honeycomb monoliths (HMs) based on an ultrathin and stiff nanoscaffold, namely a honeycomb alumina nanoscaffold (HAN), for the first time (Figure 1(Ciii)) [106]. Specifically, large-scale HAN structures were fabricated from high-purity aluminum foil through a nanoindentation–anodization–etching process. A representative HAN consists of a microminiaturized honeycomb monolith with a hexagonal cell arrangement, featuring an intercell spacing of 400 nm and an ultrathin cell wall thickness of only 16 ± 2 nm. Impressively, the cell density of the HAN reaches 4.65×10^9 cells per square inch (cpsi), which is five orders of magnitude higher than the previously reported highest value. Meanwhile, despite the ultrathin cell walls, the HAN exhibits remarkable stiffness and mechanical stability, as confirmed by nanoindentation experiments. Such robust HAN provides a stable nanostructured platform for assembling

electroactive materials for micro-supercapacitors (MSCs). Consequently, an MSC constructed with HAN-based nanoelectrodes demonstrates excellent electrochemical performance. The device delivers a maximum capacitance of 128 mF cm^{-2} at a current density of 0.5 mA cm^{-2}, along with peak energy and power densities of 160 μWh cm^{-2} and 40 mW cm^{-2}, respectively.

Overall, supercapacitor design is increasingly guided by application-specific requirements. Researchers tailor device properties through material selection, surface/structural modification of conventional electrodes, and construction of composite architectures. Meanwhile, emerging material families continue to expand the available electrode and electrolyte toolbox, enabling broader performance profiles and functionality for next-generation supercapacitors.

2.2. Assembling with Energy Harvesters

Biofuel cell (BFC)/supercapacitor hybrid devices, also termed self-charging biocapacitors, integrate bioelectrochemical energy conversion with capacitive charge storage [117–119]. Their key advantage lies in capacitive bioelectrodes, which can deliver repetitive electrical pulses and thus provide instantaneous power densities far exceeding those of BFCs. This pulse capability is particularly attractive for miniaturized power supplies intended for electrical stimulation.

As a reliable energy-supply platform for wearable electronics, biosupercapacitors combine the characteristics of biofuel cells and supercapacitors to harvest and store the energy from human's sweat. A MXene/single-walled carbon nanotube/lactate oxidase hierarchical structure was designed as a dual-functional bioanode, which not only provides a superior three-dimensional catalytic microenvironment for enzyme immobilization to harvest energy from sweat, but also offers sufficient capacitance for energy storage via the electrical double-layer capacitor mechanism (Figure 2A) [120]. A wearable biosupercapacitor was fabricated in an "island–bridge" configuration, consisting of the composite bioanode, an activated carbon/Pt cathode, a polyacrylamide hydrogel substrate, and a liquid metal conductor. The device exhibits an open-circuit voltage of 0.48 V and a high power density of 220.9 μW cm^{-2} at 0.5 mA cm^{-2}. Moreover, the device maintains compact conformal adhesion to the skin under stretching and bending conditions. After repeated stretching cycles, no significant attenuation in pulsed power output is observed.

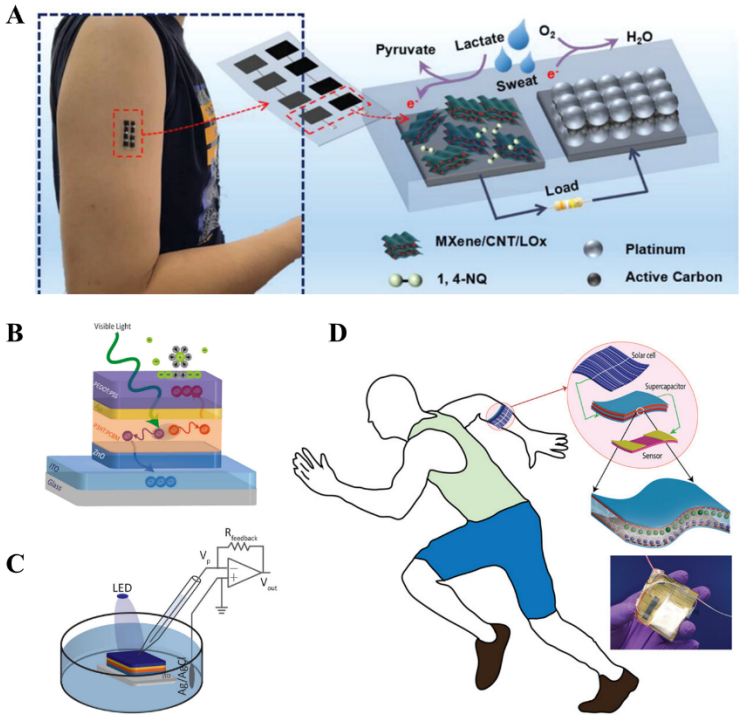

Figure 2. (**A**) Schematic illustrations of the skin-mountable BSC device [120]. Copyright 2024 Wiley-VCH. (**B**) Structure of the organic photovoltaic pseudocapacitor biointerface. It incorporates a photovoltaic unit composed of ITO/ZnO/P3HT:PCBM and a pseudocapacitor made of Au/PEDOT:PSS. (**C**) Schematic of the photocurrent measurement system [121]. Copyright 2020 American Chemical Society. (**D**) New 3D schematics and image of the hybrid structure of the self-powered system. For the fabrication of the self-powered system, a single textile SC module and a salinity sensor were placed underneath of an amorphous silicon (a-Si) flexible photovoltaic cell (Sanyo, AT7665A 664-6841) (PV) [101]. Copyright 2020 Wiley-VCH.

Organic photovoltaic (OPV) devices integrated with supercapacitors provide a promising route for wireless communication with biological systems. A wireless optoelectronic pseudocapacitor was reported that enables reversible Faradaic processes by dissociating photogenerated excitons in the OPV layer and efficiently directing holes to the supercapacitor electrode and the pseudocapacitive electrode–electrolyte interfacial layer, thereby converting light into a safe capacitive current output (Figure 2B,C) [121]. At the biointerface, the device produced a peak capacitive current of ~3 mA cm^{-2} with a total charge injection of ~1 μC cm^{-2} and a responsivity of 30 mA W^{-1}, yielding a photovoltage exceeding 400 mV. Moreover, modulation of PEDOT:PSS regulated the charge–discharge dynamics, enabling an ultrafast capacitive light response (~50 μs) and efficient membrane depolarization at the single-cell level.

To build a self-powered wearable platform, a sweat-based flexible supercapacitor (SC) and a salinity sensor were integrated beneath an amorphous silicon (a-Si) flexible photovoltaic cell (Figure 2D) [101]. During illumination, the photovoltaic cell charged the SC, leading to a rapid rise in device potential. After charging, the photovoltaic cell was disconnected. The integrated unit functioned as an energy module for the wearable system and provided sufficient stored energy to support autonomous operation of the salinity sensor. Beyond wearables, photovoltaic–supercapacitor integration has also been explored for implantable medical electronics [122]. In this design, the energy-storage supercapacitor comprised two electrodes separated by a cellulose membrane and was coupled to an external miniature solar panel for light harvesting. The device operated using electrolytes available in body fluids, enabling reliable charge–discharge behavior under physiologically relevant conditions.

3. Biocompatibility and Degradability

3.1. Biocompatibility

Different application scenarios impose different biocompatibility requirements. As the degree of contact between supercapacitors and animal or human tissues increases, the demand for biocompatibility becomes more stringent. In *in vivo* applications, mechanical mismatch and adverse biological interactions can cause device malfunction, inflammation, and even tissue damage, thereby constraining the selection of electrode materials, electrolytes, and encapsulation strategies. Most biocompatibility studies evaluate supercapacitors across multiple biological levels, including cells, tissues, organs, and whole organisms. These assessments examine whether the device induces cytotoxicity, inflammatory or immune responses, and abnormalities in organ morphology or function [123,124].

For example, an all-hydrogel micro-supercapacitor using a PANI@rGO/MXene gel electrode and a PAM–Alg hydrogel electrolyte has been reported [125]. Although the cytocompatibility of each constituent material has been validated in multiple studies, the biocompatibility of the integrated, all-in-one micro-supercapacitor still requires systematic evaluation at both cellular and *in vivo* levels. For in vitro assessment, rat cardiomyocytes (H9c2(2-1)) were selected. Culture medium was first conditioned by incubating it with the micro-supercapacitors. Conditioned extracts with concentrations ranging from 0% to 100% were then used to culture cardiomyocytes for 24 h. High cell viability (>90%) was observed in media containing 1%, 5%, 10%, 25%, and 50% extracts. Media containing 75% and 100% extracts maintained acceptable viability (>80%) (Figure 3A,B). *In vivo* biocompatibility was further evaluated by surgically implanting the all-hydrogel micro-supercapacitor onto a beating rat heart for 14 days. Systemic and local responses were assessed using biochemical and histological analyses relevant to foreign-body inflammation. Serum measurements showed no significant differences among groups in electrolytes, creatine kinase, creatinine, lactate dehydrogenase, or aspartate aminotransferase. Masson staining of heart tissue revealed comparable collagen deposition across the three groups (3.15%, 3.78%, and 2.71%), indicating no evidence of myocardial fibrosis associated with device presence or adhesion (Figure 3C,D). Immunohistochemical staining for macrophage markers CD86 (M1) and CD206 (M2) also showed no obvious differences, suggesting negligible immune response to implantation (Figure 3E–G). In addition, hematoxylin and eosin (H & E) staining indicated no apparent pathological changes in major organs, including the heart, liver, spleen, lung, and kidney.

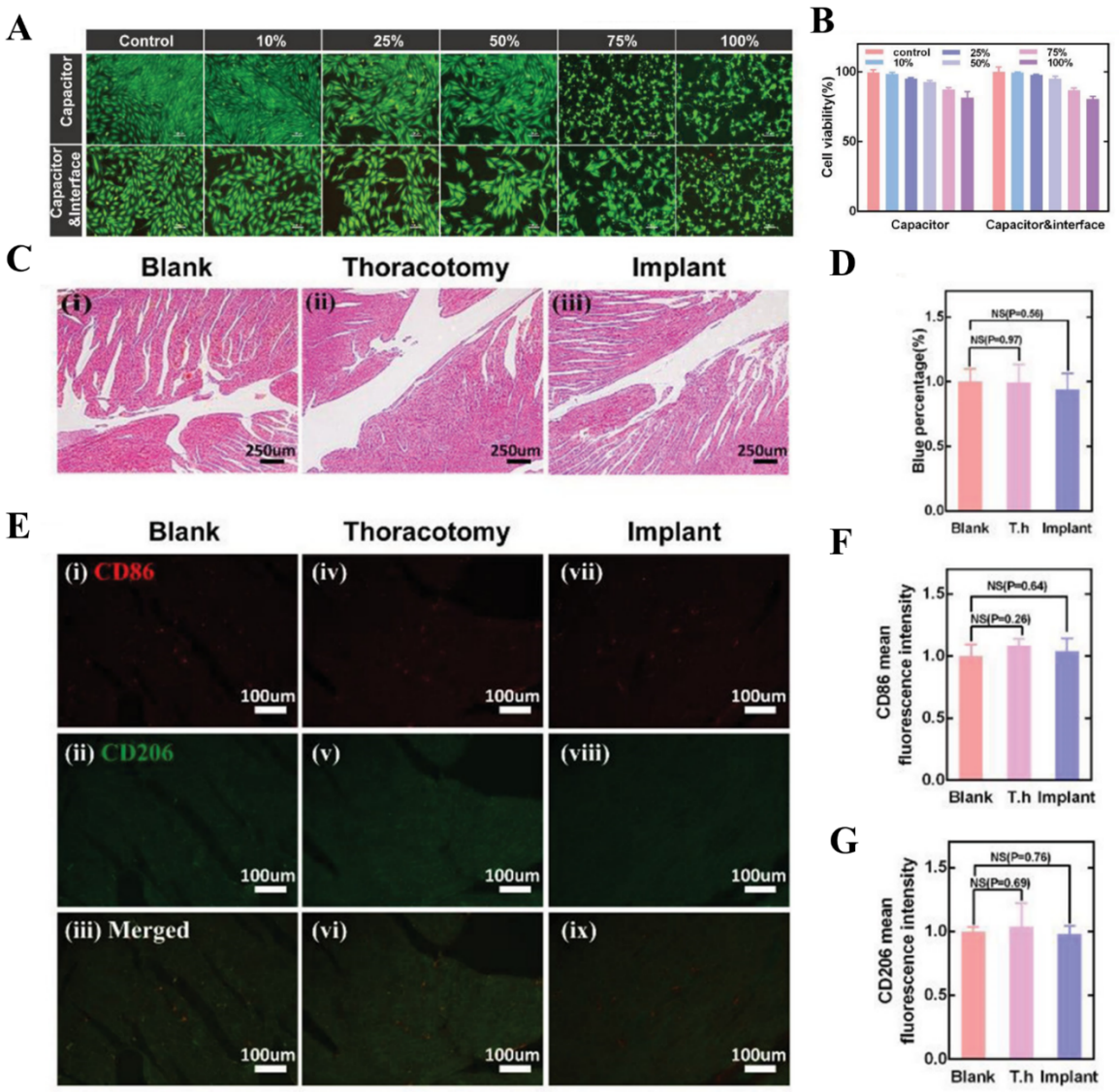

Figure 3. Biocompatibility of supercapacitors. (**A**) Fluorescent microscopic images and (**B**) plots of cell viability after co-culture of rat cardiomyocytes (H9c2(2-1)) with different percentages of extract. (**C**) Representative immunostaining images and (**D**) the degree of inflammation of heart tissues of mice in control, thoracotomy and implanted group after 14 days. (**E**) Representative immunofluorescence images and (**F**,**G**) normalized fluorescence intensities obtained from tissues of mice in control, thoracotomy and implanted group after 14 days, where green and red fluorescence correspond to the expression of macrophages M1 (CD86, f) and M2 (CD206, g) [125]. Copyright 2021 Wiley-VCH.

3.2. Degradable Supercapacitors

In many implantable scenarios, non-degradable devices require surgical retrieval, which can cause secondary trauma, increase infection risk, and impose additional clinical burden. By contrast, biodegradable designs can obviate removal surgery, mitigate long-term foreign-body responses, and allow programmable device lifetimes, making them especially valuable for temporary monitoring and short-term therapy [126,127].

The degradation of biodegradable supercapacitors generally involves both chemical dissolution and physical disintegration. For transition-metal thin-film electrodes or current collectors such as W, Mo, and Fe, the dominant chemical degradation pathways in aqueous electrolytes or PBS involve oxidation, hydrolysis, and ionization. Specifically, W and Mo can first form surface WO_x and MoO_x layers, which are subsequently converted into soluble oxyanions such as WO_4^{2-} and MoO_4^{2-}. In contrast, Fe is more prone to forming oxide/hydroxide corrosion products, including FeO_x, FeOOH, and $Fe(OH)_x$. In addition to these chemical reactions, physical processes such as water permeation, ion diffusion, electrolyte swelling or dehydration, metal/polymer interfacial delamination, and thin-film cracking can further accelerate structural failure of the device. A systematic investigation examined the dissolution kinetics of individual components in biodegradable micro-supercapacitors (MSCs) fabricated from

these materials, as well as the degradation behavior of the integrated device [128]. In this study, metal films were either exposed to NaCl/agarose gel or immersed in PBS. The thickness of the metal layers was monitored over time, and linear fitting was applied to extract the dissolution rates of each metal (Figure 4A,B). The degradation behavior of the NaCl/agarose gel electrolyte and Mo interdigitated electrodes was also characterized (Figure 4C,D). Based on these results, a fully biodegradable supercapacitor was demonstrated as a transient power source for bioimplantable systems. In addition to these materials, cellulose-based hydrogels, poly(1,8-octanediol-co-citrate) (POC), polyester polymers, polylactic acid (PLA), and polylactic acid copolymers have also been explored as biodegradable electrolytes or encapsulation materials for supercapacitors. Degradable electrolytes should exhibit high ionic conductivity, good electrode wettability, and an appropriate electrochemical stability window [129,130]. Meanwhile, their salt concentration, pH, osmolality, and degradation products should be carefully controlled to avoid significant tissue irritation. Polymer encapsulation layers are primarily used to regulate the ingress of water and ions, thereby determining the functional lifetime of the device. Ideal encapsulation materials should possess low water permeability, good film-forming capability, electrical insulation, strong interfacial adhesion with electrodes/electrolytes/substrates, flexibility compatible with soft tissues, and predictable degradation kinetics [131–133]. Therefore, materials design should balance structural stability during device operation with rapid degradation and bioresorption after completion of the intended function.

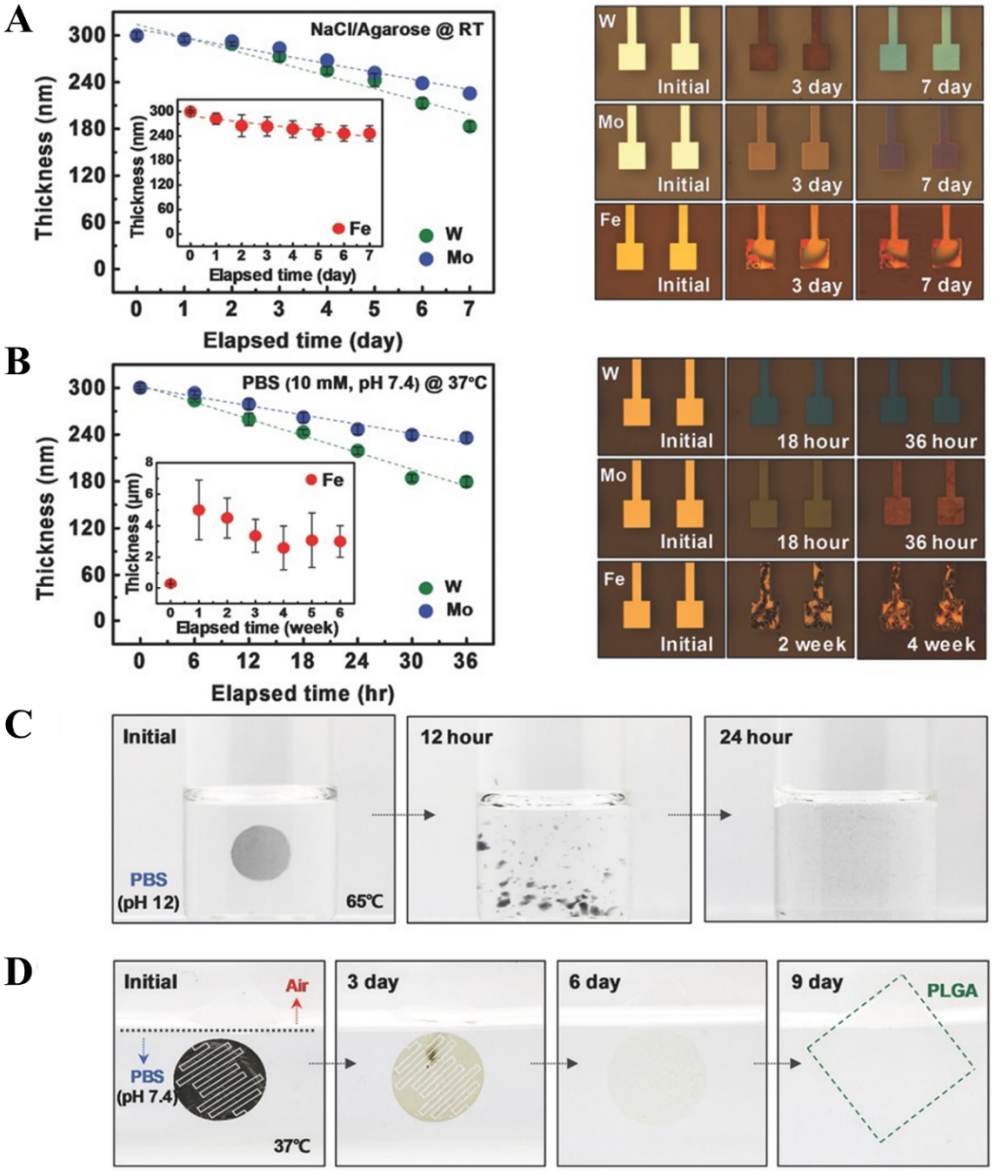

Figure 4. Degradability of supercapacitors. (**A**,**B**) Dissolution kinetics (left) and optical images (right) of bioabsorbable metal films (300 nm thick W, Fe and Mo) measured at different times with NaCl/Agarose gel on top at room temperature and in phosphate buffered saline (PBS; 10 × 10^{-3} M, 37 °C, pH 7.4). (**C**) Time-series photographs of NaCl/Agarose gel electrolyte samples in PBS (pH 12) at 65 °C. (**D**) Optical images of the dissolution of Mo interdigital electrodes immersed in PBS (pH 7.4) at 37 °C [128]. Copyright 2017 Wiley-VCH.

Researchers have further extended the concept of biodegradable supercapacitors to edible systems by proposing a template-imprinting strategy for edible miniature supercapacitors (EMSCs), in which all electrode and electrolyte components are ingestible, swallowable, and nontoxic to humans [134]. In this approach, commercially available food products and green food additives were employed as electrode materials. The resulting EMSCs exhibited high mechanical robustness and flexibility, enabling them to adapt to diverse environments and to be printed onto substrates of arbitrary shapes, including planar and non-planar polymer surfaces such as skin, fruit, and bread. In addition, the devices demonstrated competitive electrochemical performance, delivering an energy density of 10.86 μWh cm^{-2} and a power density of 0.78 mW cm^{-2}. Owing to their flexibility and structural integrity, EMSCs could even be rolled into gelatin drug capsules to serve as real-time power sources for capsule endoscopy.

In practical biomedical applications, the degradation behavior and lifetime of supercapacitors are critical considerations. Achieving controllable degradation profiles remains a key challenge. A fully bioabsorbable capacitor (BC) has been reported, employing a biodegradable Fe film as the current collector [135]. By selecting different encapsulation materials, such as poly (vinyl alcohol) (PVA) for short-term operation and polylactic acid (PLA) for longer-term stability, the device achieved tunable functional lifetimes, enabling application-specific working durations.

4. Supercapacitors for *In Vivo* Analysis

4.1. Wearable Supercapacitors

Wearable electronics are developing rapidly and offer practical solutions for real-time patient monitoring, emergency management, and daily self-health management. Wearable bioelectronic systems powered by stretchable supercapacitors can be mounted directly on skin or integrated into textiles, shoes, and other accessories. Depending on the level of biointerface interaction, wearable devices are commonly classified into three categories: non-contact, skin-contact, and skin-adhering. From a fabrication perspective, the design of wearable supercapacitors should balance electrochemical performance with mechanical deformability, interfacial stability, and manufacturability. Electrode materials and current collectors should provide efficient electron transport, sufficient electrochemically active surface area, and strong adhesion to flexible or stretchable substrates. Structural designs such as fiber/yarn configurations, serpentine layouts, prestrained wavy structures, coiled geometries, and buckled architectures are often employed to accommodate body motion while maintaining stable capacitance. In addition, gel or solid-state electrolytes and encapsulation layers should minimize leakage, improve safety, and preserve device performance under repeated bending, stretching, and twisting [136,137].

Non-contact wearables can be integrated into clothing, gloves, wristbands, or shoes through appropriate structural designs to achieve application-specific functions. Yarn-type supercapacitors (SCs) are particularly attractive for such systems because they are flexible, weavable, lightweight, and compatible with scalable, low-cost fabrication, enabling efficient on-textile energy storage. A functionalized stainless-steel (FSS) yarn platform was reported for an all-solid-state asymmetric yarn SC [138]. In this design, a Ni–Co–S layer was deposited onto FSS yarn by one-step electrodeposition as the positive electrode, while graphene oxide on FSS yarn was reduced to serve as the negative electrode. A LiOH/PVA gel acted as both the solid-state electrolyte and separator, yielding a fully solid asymmetric yarn SC. The device exhibited high flexibility and mechanical robustness, maintaining stable performance under tensile strain up to 100%. It also delivered a power density of 0.553 mW cm^{-2} (129.1 mW cm^{-3}) and an energy density of 0.0487 mWh cm^{-2} (10.19 mWh cm^{-3}). The yarn SCs were further inserted into elastic PDMS tubes to form stretchable SCs. A cable-type SC array (two in series and four in parallel) was then integrated into fabric to power LEDs (Figure 5A). However, despite its promising textile compatibility and stretchability, the long-term stability of the FSS yarn-based device under sweat exposure, repeated washing, and complex multiaxial deformation remains to be further verified.

Beyond electrochemical performance, wearable supercapacitors should also provide comfort, breathability, and durability under repeated deformation. As shown in Figure 5B, a substrate-free, self-contained, breathable three-dimensional supercapacitor was fabricated using veil electrodes based on activated carbon fibers (ACF) [139]. The highly porous conductive veil electrodes enabled a lightweight, breathable, flexible, foldable, and customizable device with an energy density of 5.52 Wh kg^{-1}. The supercapacitor maintained >86.6% capacitance retention over 10,000 charge–discharge cycles under mechanical deformations such as folding, cutting, and compression. It also withstood compressive stresses of ~176.2 MPa. When placed beneath an insole, the device was able to power electronic components under body-weight loading.

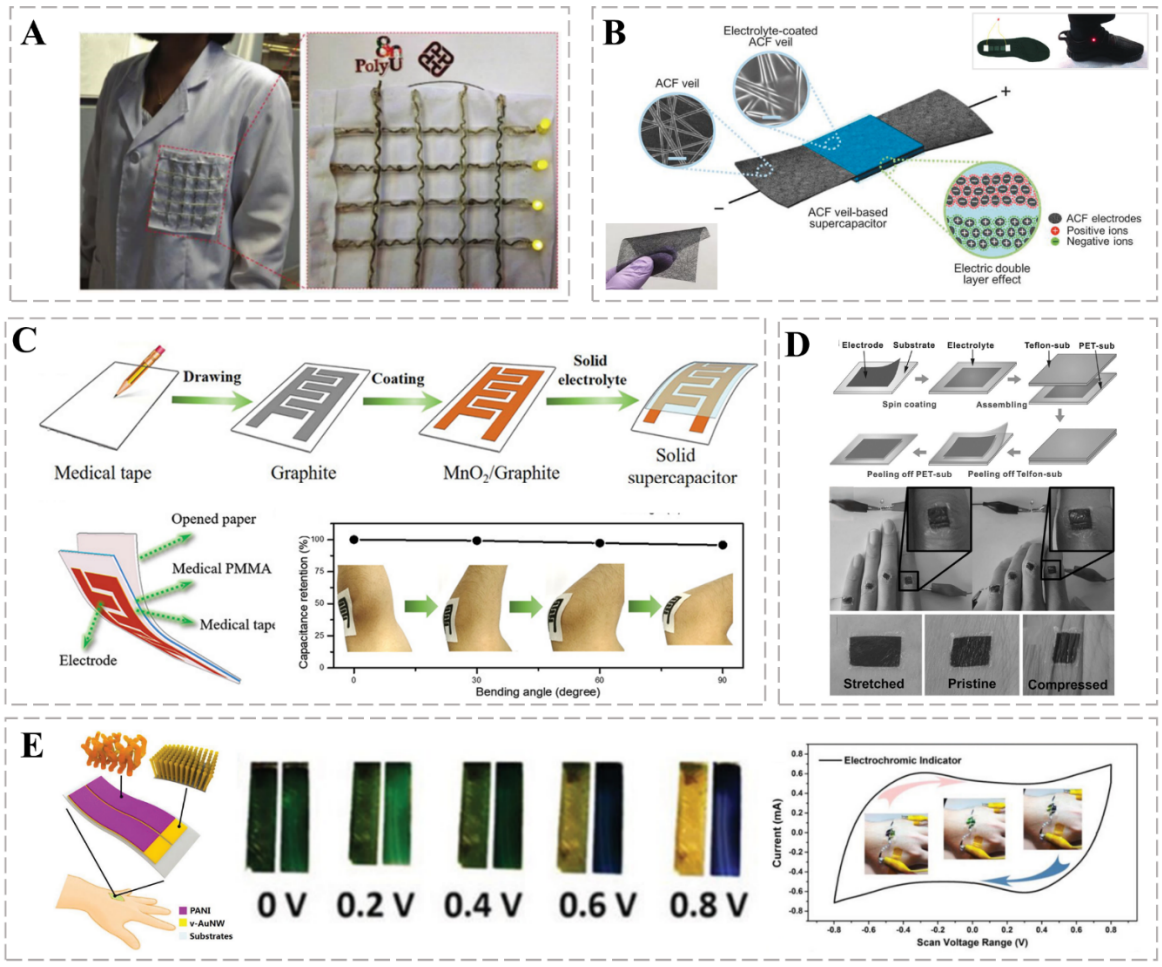

Figure 5. Wearable supercapacitors. (**A**) Array of yarn supercapacitors (SCs) integrated on clothing [138]. Copyright 2018 Wiley-VCH. (**B**) Supercapacitors based on activated carbon fiber (ACF) veil electrodes were connected under the insole to power the red LEDs [139]. Copyright 2018 Wiley-VCH. (**C**) Medical tape-based integrated gypsum-like micro-supercapacitors [140]. Copyright 2019 Wiley-VCH. (**D**) Epidermal supercapacitors (SC-E). A higher voltage could be obtained by using four SC-Es in series to power the red LED [141]. Copyright 2016 Wiley-VCH. (**E**) Electrochromic supercapacitors based on v-AuNW/PANI patterned electrodes, showing different electrode colors under different charge states [142]. Copyright 2019 Wiley-VCH.

Compared with non-contact wearables, skin-contact devices operate in direct contact with the epidermis and therefore impose more stringent requirements on biocompatibility, skin adhesion, and mechanical compliance. In practice, soft, skin-friendly substrates and adhesives are commonly employed to laminate stretchable supercapacitors onto the skin while maintaining conformal contact during daily motion. As shown in Figure 5C, plaster-like micro-supercapacitors integrated with medical adhesive tape were reported using a simple pencil-drawing method combined with mild MnO_2 solution deposition [140]. In this design, planar thin-film micro-supercapacitors (TFMSCs) were constructed on flexible medical tape with strong skin adhesion. A highly bendable and stretchable medical tape served as the microstructural support, while a medical-grade polymethyl methacrylate (MPMMA) layer was introduced to improve skin compatibility. These plaster-like supercapacitors could be mounted directly onto human skin via a straightforward "lift-and-fix" procedure. They also exhibited excellent mechanical durability during joint motion, retaining over 90% of their capacitance after 200 bending cycles while the elbow was repeatedly flexed from 0° to 90°. However, the reported bending test of 200 cycles is still limited and require further improvement.

The rapid growth of wearable electronics has driven intensive research into epidermal devices that can be laminated directly onto skin while integrating functions such as communication, health monitoring, and signal processing. Skin-adhering wearables impose stricter requirements on biocompatibility, breathability, and long-term wearing comfort. These demands make electrode/material optimization and scalable, non-destructive assembly strategies key challenges in developing practical epidermal supercapacitors (SC-Es) for intelligent and

self-powered systems. As shown in Figure 5D, an ultrathin, free-standing supercapacitor with a thickness of ~1 μm and excellent power capability was reported for epidermal electronics [141]. A hybrid single-walled carbon nanotube/poly(3,4-ethylenedioxythiophene) (SWCNT/PEDOT) film served as a highly conductive ultrathin electrode. To enable device release without structural damage, a stepwise stripping method was developed using two substrates with different surface energies, allowing the integrated ultrathin supercapacitor to be delaminated in a controlled manner. The resulting devices exhibited outstanding mechanical robustness, maintaining performance over 10^5 bending cycles, while delivering a high-power density of 332 kW kg^{-1} and a short response time of 11.5 ms. By connecting four SC-Es in series, higher output voltages were achieved to power red light-emitting diodes (LEDs). When mounted on a finger, the SC-E followed bending and straightening motions without noticeable performance degradation, highlighting its potential as an epidermal power source for wearable electronics. However, large-area fabrication, transfer yield, and packaging reliability remain major challenges for its practical application.

The versatility of supercapacitors, including electrochromism and degradability, is gradually being incorporated into next-generation wearable biodevices. In electrochromic supercapacitors, the electrode color changes under different applied voltages, enabling direct visual monitoring of the energy state. Polyaniline (PANI) has been widely used for this purpose because of its relatively high electrical conductivity, high pseudocapacitance, flexibility, and reversible color switching between green and blue during redox processes. As shown in Figure 5E, v-AuNWs grown on antiseptic films served as a soft, skin-friendly current collector, while deposited PANI provided pseudocapacitance; the resulting v-AuNW/PANI patterned electrodes could be conveniently attached to human skin using adhesive tape [142]. In the uncharged state, both electrodes appeared green. When the potential was scanned to +0.8 V at 100 mV s^{-1}, the positively charged electrode gradually turned dark blue, whereas the negatively charged electrode gradually changed to light yellow. The areal specific capacitance reached 11.76 mF cm^{-2} at a scan rate of 10 mV s^{-1}, and the areal energy density reached 0.71 μWh cm^{-2} at a power density of 40 μW cm^{-2}. These results indicate that the wearable supercapacitor shows potential for future applications in soft skin electronics.

4.2. Implantable Devices

An important application of bioelectronics is to enable real-time *in vivo* health monitoring and medical intervention via implanted functional devices, such as radio transmitters [143], automatic drug delivery systems [144], sensors [145,146], pacemakers [147], deep brain stimulators and diagnostic/therapeutic devices. To operate reliably in the human body, implantable supercapacitors require the seamless integration of biocompatible electrodes, electrolytes, substrates, and encapsulation materials, along with long-term electrochemical stability, leakage prevention, sterilization compatibility, and mechanical matching with soft tissues.

Kim's team demonstrated a flexible fibrous bio-supercapacitor based on an NAD^+ redox system [148]. The yarn electrodes were fabricated by a double-winding process and then inserted into host CNT sheets, which were loaded with NAD^+ and benzoquinone (BQ) as guests. To evaluate their potential as implantable energy-storage units, the electrochemical performance of the NAD/BQ/CNT yarn supercapacitors was tested in commonly used model biological fluids, including PBS, HBSS, saline, and serum, and all exhibited the expected electrochemical behavior. The areal capacitance reached 55.73 mF cm^{-2} in PBS, with an area energy density of 19.81 μWh cm^{-2} and an area power density of 446 W cm^{-2}. Two flexible yarn electrodes were sutured in parallel into the abdominal cavity of rats, and the supercapacitor implanted in subcutaneous tissue exhibited electrochemical performance similar to that measured in PBS and showed significant biocompatibility (Figure 6A–C). Nevertheless, despite its promising biofluid compatibility and implantability, the long-term stability of the redox mediators, potential BQ leakage, persistence of CNT components, and chronic tissue responses require further systematic investigation.

In addition, a fully biodegradable and bioabsorbable high-performance supercapacitor implant was reported [149]. Two-dimensional amorphous molybdenum oxide (MoO_x) flakes were used as electrodes and grown in situ on water-soluble molybdenum foil via a green electrochemical strategy. The device was lightweight and thin, offering mechanical flexibility, adjustable degradation duration, and good biocompatibility. It also delivered a high areal capacitance of 112.5 mF cm^{-2} at 1 mA cm^{-2} and an area energy density of 15.64 μWh cm^{-2}. During degradation, the outer packaging layer was fully absorbed by metabolism after one month, accompanied by leakage of inner MoO_x flakes and electrolyte from the edges of the broken implant (Figure 6D). Residual implant materials were observable in the subcutaneous region after three months, completely dissolved and disappeared after six months, and no inflammatory response was observed during device degradation (Figure 6E). After subcutaneous implantation on the dorsal side of Sprague–Dawley (SD) rats, the encapsulated biodegradable supercapacitor successfully powered a red LED (threshold voltage 1.5 V) after charging (Figure 6F). These pioneering studies demonstrate the potential of supercapacitors for implantable bioelectronics. Nevertheless, the edge leakage of

MoO_x flakes and electrolyte during encapsulation degradation suggests that more precise control over dissolution pathways, degradation uniformity, and local by-product release remains necessary for reliable transient implants. More broadly, the development of implantable supercapacitors is shifting from demonstrating basic functionality in bodily fluids toward ensuring safe, stable, and controllable operation *in vivo* during the intended functional lifetime. Future research should therefore move beyond the pursuit of higher areal capacitance or energy density and place greater emphasis on the synergistic optimization of device-level reliability, degradation predictability, and biosafety.

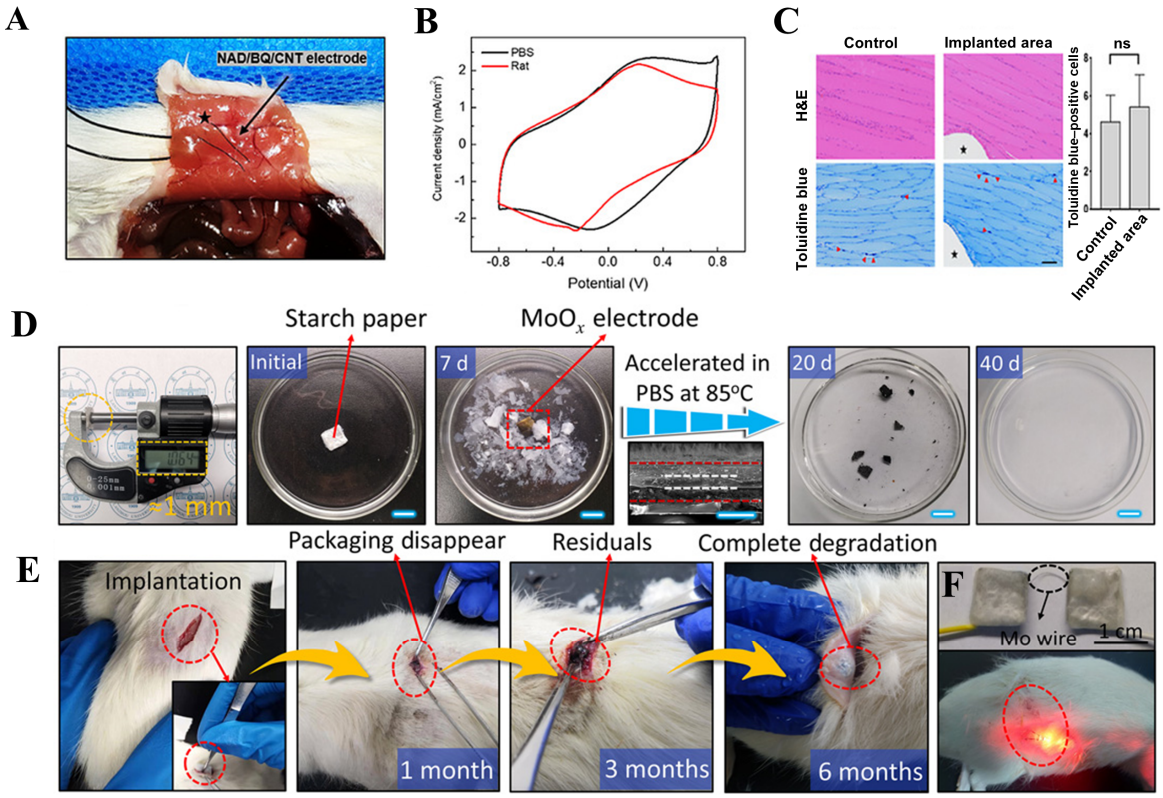

Figure 6. Implantable Devices. (**A**) Photograph of the NAD/BQ/CNT yarn supercapacitor implanted into the abdominal cavity of a rat. (**B**) Comparison of the CV graphs of the performance of the NAD supercapacitor in PBS and implanted in a rat. (**C**) Histological analysis by H&E and toluidine blue staining in control and implanted tissues [148]. Copyright 2021 Wiley-VCH. (**D**) Photographs of the encapsulated supercapacitor implant with ~1 mm thickness at various dissolution stages in PBS solution. (**E**) *In vivo* degradation evaluation of the supercapacitor implant in the subcutaneous area of SD rats. (**F**) Encapsulated supercapacitor implants in series connected with the biodegradable Mo wire and a red LED light powered by the implanted supercapacitors in series [149]. Copyright 2021 American Association for the Advancement of Science.

4.3. Supercapacitors for Neural and Tissue Stimulation

Bioelectronics enables deeper understanding of biodynamics and biological functions and offers significant therapeutic potential for a range of diseases, including Parkinson's disease, congenital heart defects, and paralysis [150]. However, conventional macroscale bioelectronic devices are typically rigid and can mechanically irritate or damage cells and tissues, which hinders the formation of conformal cellular and subcellular biointerfaces. For next-generation bioelectronic systems, establishing large-area, mechanically compliant biointerfaces is essential to reduce mechanical mismatch and minimize biocompatibility-related complications [151–153].

Recently, an implantable in-hydrogel wireless supercapacitor-activated neuron system (W-SCAN) composed of a wireless coil, diode bridge circuit, in-hydrogel supercapacitor, and stimulation electrodes was developed to provide bidirectional and tunable ion-diffusion currents for safe excitation or inhibition of brain neurons (Figure 7A) [154]. The device achieves a wireless transmission efficiency (WTE) of 75%, maintaining approximately 50% WTE after subcutaneous implantation and 96.7% performance retention after seven days *in vivo*. Benefiting from the in situ radical addition mechanism, the in-hydrogel supercapacitor exhibits a charge-storage capability approximately 90 times higher than that of devices without hydrogel encapsulation. Owing to its good biocompatibility and minimal tissue irritation, the W-SCAN system can function as a wireless energy transmission terminal for ion-oscillation

stimulation of targeted brain regions. By implanting the electrodes into the thalamus, amygdala, and prefrontal cortex, the system successfully modulates neural potential intensity and frequency via an external charging coil, demonstrating the potential of multimodule supercapacitors for the treatment of neurological disorders such as Parkinson's disease, severe depression, and Alzheimer's disease.

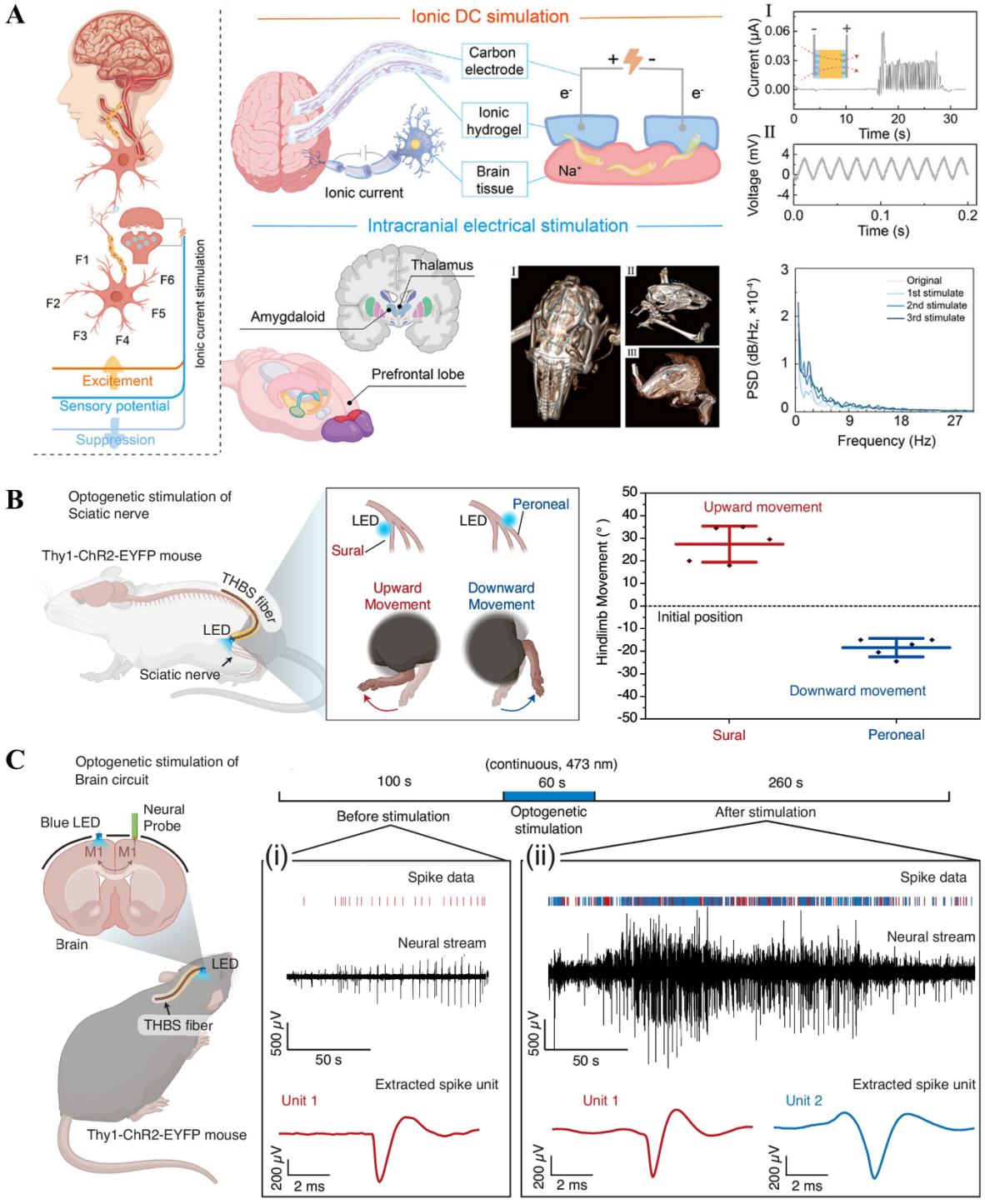

Figure 7. (**A**) The applications of W-SCAN as a medium for intracranial targeted ion electrical stimulation [154]. Copyright 2025 Wiley-VCH. (**B**) Left: Schematic illustrating optogenetic stimulation of the sciatic nerve in a mouse (PNS application). Right: Hindlimb movement angles induced by optogenetic stimulation via THBS fibers targeting the sural or peroneal branch of the sciatic nerve. (**C**) Left: Schematic illustrating optogenetic stimulation of the M1–M1 circuit in a mouse brain. Right: Neuronal activity in contralateral M1 cortex before (**i**) and after (**ii**) THBS fibers induced optogenetic stimulation in M1 cortex [96]. Copyright 2025 Springer Nature.

The Seongjun Park team presented a tough hydrogel-based supercapacitor (THBS) fiber that integrates all components—electrodes, electrolyte, current collectors, and encapsulation—into a single, unified, and mechanically robust fiber-shaped architecture [96]. The THBS fiber achieved a maximum areal capacitance of 268 mF/cm^2 and volumetric capacitance of 18.8 F/cm^3 at a current density of 1.0 mA/cm^2, an areal energy density of 29.8 $\mu Wh/cm^2$, and an areal power density of 8.48 mW/cm^2. It also exhibited exceptional mechanical and electrochemical stability during repeated deformation, simulating the dynamic conditions of *in vivo* implantation. Long-term functionality was confirmed over five weeks with minimal immune response. To demonstrate the *in vivo* applicability of the THBS fibers, the researchers employed them as an energy source for optogenetic stimulation of both the peripheral and central nervous systems (CNS) (Figure 7B,C). *In vivo* implantation demonstrated successful LED operation in a freely moving mouse and enabled effective optogenetic stimulation of these neural systems. THBS fibers have broad application potential in the field of bioelectronics and are expected to be integrated into various medical devices.

These studies illustrate the transition of implantable supercapacitors from passive energy-storage units to active biointerface modules for neural modulation. However, the wireless transmission efficiency of W-SCAN decreased to approximately 50% after implantation, and its 7-day *in vivo* stability is still insufficient to support chronic therapeutic applications. In contrast, the THBS fiber, which maintained functionality for five weeks *in vivo* with minimal immune response, represents an important advance in soft implantable energy-storage devices. Nevertheless, its long-term durability under chronic implantation remains to be further validated. Future studies should therefore move beyond short-term proof-of-concept demonstrations and focus on chronic neural safety, stable charge delivery, tissue responses, wireless power reliability, and integration with closed-loop bioelectronic systems.

5. Summary and Prospect

In conclusion, this review summarizes recent design strategies for supercapacitors and highlights their latest progress in *in vivo* analysis applications. We first discuss materials selection and architectural design, with brief coverage of representative one-dimensional (1D) fiber, two-dimensional (2D) planar, and three-dimensional (3D) stereoscopic supercapacitors. To achieve specific functions and further enhance device performance, diverse composite electrode materials and solid/hydrogel electrolytes have been developed to meet practical requirements, and supercapacitor architectures are becoming increasingly versatile.

For wearable and implantable applications, biocompatibility is a fundamental prerequisite. In some scenarios, additional requirements such as degradability or bioresorbability are desirable, which further restrict the choice of electrode, electrolyte, and encapsulation materials and accelerate the exploration of emerging material systems. Driven by the growing demand for health monitoring, wearable supercapacitors have been implemented in formats such as textiles, watch straps, and electronic skins, demonstrating strong potential for next-generation bioelectronics in human health monitoring. Finally, porous carbon-based micro-supercapacitors have been demonstrated for capacitive charge–discharge operation or conventional pulsed-current modulation across in vitro, acute ex vivo, and acute *in vivo* settings, while maintaining long-term stability and reasonable biocompatibility. These advances indicate promising prospects for supercapacitor-enabled bioelectronic therapy.

Author Contributions

Y.L.: conceptualization, literature search, writing—original draft preparation; J.J.: literature screening, data curation; C.H.: visualization; T.L.: supervision, writing—review and editing; L.Z.: conceptualization, funding acquisition, writing—review and editing. All authors have read and agreed to the published version of the manuscript.

Funding

This research was funded by the Natural Science Foundation of China grant number 22022402 and the Postdoctoral Fellowship Program of CPSF grant number GZC20240477.

Conflicts of Interest

The authors declare no conflict of interest.

Use of AI and AI-Assisted Technologies

No AI tools were utilized for this paper.

References

1. Madsen, K.E.; Flavin, M.T.; Rogers, J.A. Materials advances for distributed environmental sensor networks at scale. *Nat. Rev. Mater.* **2026**, *11*, 26–49.
2. Gong, S.; Lu, Y.; Yin, J.; et al. Materials-driven soft wearable bioelectronics for connected healthcare. *Chem. Rev.* **2024**, *124*, 455–553.
3. Mahato, K.; Saha, T.; Ding, S.; et al. Hybrid multimodal wearable sensors for comprehensive health monitoring. *Nat. Electron.* **2024**, *7*, 735–750.
4. Wang, L.; Xie, S.; Wang, Z.; et al. Functionalized helical fibre bundles of carbon nanotubes as electrochemical sensors for long-term *in vivo* monitoring of multiple disease biomarkers. *Nat. Biomed. Eng.* **2019**, *4*, 159–171.
5. Xie, Z.; Avila, R.; Huang, Y.; et al. Flexible and stretchable antennas for biointegrated electronics. *Adv. Mater.* **2020**, *32*, 1902767.
6. Huang, Z.; Hao, Y.; Li, Y.; et al. Three-dimensional integrated stretchable electronics. *Nat. Electron.* **2018**, *1*, 473–480.
7. Someya, T.; Bao, Z.; Malliaras, G.G. The rise of plastic bioelectronics. *Nature* **2016**, *540*, 379–385.
8. Park, T.; Lee, D.Y.; Ahn, B.J.; et al. Implantable anti-biofouling biosupercapacitor with high energy performance. *Biosens. Bioelectron.* **2024**, *243*, 115757.
9. Jiang, L.; Lu, X. Functional hydrogel-based supercapacitors for wearable bioelectronic devices. *Mater. Chem. Front.* **2021**, *5*, 7479–7498.
10. Dissanayake, K.; Kularatna-Abeywardana, D. A review of supercapacitors: Materials, technology, challenges, and renewable energy applications. *J. Energy Storage* **2024**, *96*, 112563.
11. Muralee Gopi, C.V.V.; Alzahmi, S.; Narayanaswamy, V.; et al. Supercapacitors: A promising solution for sustainable energy storage and diverse applications. *J. Energy Storage* **2025**, *114*, 115729.
12. Lim, J.M.; Jang, Y.S.; Nguyen, H.V.T.; et al. Advances in high-voltage supercapacitors for energy storage systems: Materials and electrolyte tailoring to implementation. *Nanoscale Adv.* **2023**, *5*, 615–626.
13. Shalini, S.; Naveen, T.B.; Durgalakshmi, D.; et al. Progress in flexible supercapacitors for wearable electronics using graphene-based organic frameworks. *J. Energy Storage* **2024**, *86*, 111260.
14. Pacchioni, G. Sustainable flexible supercapacitors. *Nat. Rev. Mater.* **2022**, *7*, 844.
15. Zhou, S.; Zhao, Y.; Zhang, K.; et al. Impact-resistant supercapacitor by hydrogel-infused lattice. *Nat. Commun.* **2024**, *15*, 6481.
16. Gopi, C.V.V.M.; Alzahmi, S.; Narayanaswamy, V.; et al. A review on electrode materials of supercapacitors used in wearable bioelectronics and implantable biomedical applications. *Mater. Horiz.* **2025**, *12*, 4092–4132.
17. Ramachandran, T.; Sana, S.S.; Kumar, K.D.; et al. Asymmetric supercapacitors: Unlocking the energy storage revolution. *J. Energy Storage* **2023**, *73*, 109096.
18. Liu, X.; Liu, C.-F.; Xu, S.; et al. Porous organic polymers for high-performance supercapacitors. *Chem. Soc. Rev.* **2022**, *51*, 3181–3225.
19. Dong, W.; Xie, M.; Zhao, S.; et al. Materials design and preparation for high energy density and high power density electrochemical supercapacitors. *Mater. Sci. Eng. R Rep.* **2023**, *152*, 100713.
20. Wang, Y.; Song, Y.; Xia, Y. Electrochemical capacitors: Mechanism, materials, systems, characterization and applications. *Chem. Soc. Rev.* **2016**, *45*, 5925–5950.
21. Kim, H.J.; Koo, J.H.; Lee, S.; et al. Materials design and integration strategies for soft bioelectronics in digital healthcare. *Nat. Rev. Mater.* **2025**, *10*, 654–673.
22. Zhang, H.; Li, A.; Liu, Y.-F.; et al. Spinal TAOK2 contributes to neuropathic pain via cGAS-STING activation in rats. *iScience* **2023**, *26*, 107792.
23. Hu, M.; Liang, C.; Wang, D. Implantable bioelectrodes: Challenges, strategies, and future directions. *Biomater. Sci.* **2024**, *12*, 270–287.
24. Lu, T.; Ji, S.; Jin, W.; et al. Biocompatible and Long-Term Monitoring Strategies of Wearable, Ingestible and Implantable Biosensors: Reform the Next Generation Healthcare. *Sensors* **2023**, *23*, 2991.
25. Yu, M.; Kim, Y.; Nam, S.; et al. Integrated implantable bioelectronic system based on intrinsically stretchable and conductive nanocomposites. *Health Nanotechnol.* **2025**, *1*, 12.
26. Li, J.; Yang, X. Advances in bioelectronics for neural interfacing. *MRS Commun.* **2025**, *15*, 1255–1268.
27. Yamagishi, K.; Lee, S.; Yokota, T.; et al. Soft, flexible, and stretchable platforms for tissue-interfaced bioelectronics. *Adv. Sci.* **2026**, *13*, e21521.
28. Oh, S.; Lee, S.; Kim, S.W.; et al. Softening implantable bioelectronics: Material designs, applications, and future directions. *Biosens. Bioelectron.* **2024**, *258*, 116328.
29. Le Floch, P.; Zhao, S.; Liu, R.; et al. 3D spatiotemporally scalable *in vivo* neural probes based on fluorinated elastomers. *Nat. Nanotechnol.* **2024**, *19*, 319–329.

30. Wang, S.; Jiang, Q.; Liu, H.; et al. Mechanically adaptive and deployable intracortical probes enable long-term neural electrophysiological recordings. *Proc. Natl. Acad. Sci. USA* **2024**, *121*, e2403380121.
31. Theocharidis, G.; Veves, A. Greater foreign-body responses to big implants. *Nat. Biomed. Eng.* **2023**, *7*, 1340–1342.
32. Wu, J.; Deng, J.; Theocharidis, G.; et al. Adhesive anti-fibrotic interfaces on diverse organs. *Nature* **2024**, *630*, 360–367.
33. Li, N.; Kang, S.; Liu, Z.; et al. Immune-compatible designs of semiconducting polymers for bioelectronics with suppressed foreign-body response. *Nat. Mater.* **2026**, *25*, 124–132.
34. Beatty, R.; Mendez, K.L.; Schreiber, L.H.J.; et al. Soft robot–mediated autonomous adaptation to fibrotic capsule formation for improved drug delivery. *Sci. Robot.* **2023**, *8*, eabq4821.
35. Mariello, M.; Kim, K.; Wu, K.; et al. Recent advances in encapsulation of flexible bioelectronic implants: Materials, technologies, and characterization methods. *Adv. Mater.* **2022**, *34*, 2201129.
36. Boufidis, D.; Garg, R.; Angelopoulos, E.; et al. Bio-inspired electronics: Soft, biohybrid, and "living" neural interfaces. *Nat. Commun.* **2025**, *16*, 1861.
37. Xie, R.; Han, F.; Yu, Q.; et al. A movable long-term implantable soft microfibre for dynamic bioelectronics. *Nature* **2025**, *645*, 648–655.
38. Jiang, X.; Wang, M.; Shang, Y.; et al. Stretchable high-capacitance supercapacitors enabled by Soft-Pore-Array engineered Ag@polyurethane current collectors. *Chem. Eng. J.* **2025**, *523*, 168489.
39. Wang, R.; Lei, D.; Zhang, H.; et al. An interface-integrated hydrogel for all-in-one flexible supercapacitor with excellent wide-temperature and self-healing properties. *Compos. Part B Eng.* **2024**, *275*, 111345.
40. Fu, K.; Zhang, X.; Lu, X.; et al. Self-healing hydrogels in flexible energy storage devices: Mechanisms, applications, and prospects. *J. Mater. Chem. A* **2026**, *14*, 1422–1449.
41. Chandrasekar, J.; Venkatesan, M.; Sun, T.-W.; et al. Recent progress in self-healable energy harvesting and storage devices—A future direction for reliable and safe electronics. *Mater. Horiz.* **2024**, *11*, 1395–1413.
42. Chen, Y.; Jin, H.; Zhang, J.; et al. Stretchable flexible fiber supercapacitors for wearable integrated devices. *J. Mater. Chem. A* **2024**, *12*, 18958–18967.
43. Shaikh, S.; Kamangar, S.; Badruddin, I.A.; et al. Towards sustainable electronics: Advances in flexible supercapacitors for energy storage applications. *J. Electroanal. Chem.* **2026**, *1000*, 119639.
44. Ding, J.; Yang, Y.; Poisson, J.; et al. Recent advances in biopolymer-based hydrogel electrolytes for flexible supercapacitors. *ACS Energy Lett.* **2024**, *9*, 1803–1825.
45. Yang, J.; Wang, M.; Chen, T.; et al. Tough, self-healable, antifreezing and redox-mediated gel polymer electrolyte with three-role $K_3[Fe(CN)]_6$ for wearable flexible supercapacitors. *Sci. China Mater.* **2023**, *66*, 1779–1792.
46. Li, B.; Bailey, J.; Yoon, S.; et al. Self-healing polymer-clay nanocomposite hydrogel-based all-in-one stretchable supercapacitor. *J. Power Sources* **2025**, *626*, 235746.
47. Lee, S.; Silva, S.M.; Aguilar, L.M.C.; et al. Biodegradable bioelectronics for biomedical applications. *J. Mater. Chem. B* **2022**, *10*, 8575–8595.
48. Huang, C.; Li, P.; Niu, X.; et al. Transient energy storage devices for implantable medical electronics. *Sci. China Mater.* **2026**, *69*, 675–699.
49. Corsi, M.; Bellotti, E.; Surdo, S.; et al. Implantable bioresorbable electronic systems for sustainable precision medicine. *Nat. Rev. Electr. Eng.* **2025**, *2*, 572–583.
50. Kim, G.; Hong, M.; Lee, Y.; et al. Biodegradable materials and devices for neuroelectronics. *MRS Bull.* **2023**, *48*, 518–530.
51. Baburaj, A.; Banerjee, S.; Aliyana, A.K.; et al. Biodegradable based TENGs for self-sustaining implantable medical devices. *Nano Energy* **2024**, *127*, 109785.
52. Ma, Y.; Sheng, H.; Zhang, H.; et al. Recent advances in biodegradable implantable electrochemical energy storage devices. *Sci. Sin. Technol.* **2024**, *54*, 786–802.
53. Kim, H.; Rigo, B.; Wong, G.; et al. Advances in wireless, batteryless, implantable electronics for real-time, continuous physiological monitoring. *Nano-Micro Lett.* **2023**, *16*, 52.
54. Chu, Z.; Zhou, Y.; Li, S.; et al. Implantable medical electronic devices: Sensing mechanisms, communication methods, and the biodegradable future. *Appl. Sci.* **2025**, *15*, 7599.
55. Cho, M.; Han, J.-K.; Suh, J.; et al. Fully bioresorbable hybrid opto-electronic neural implant system for simultaneous electrophysiological recording and optogenetic stimulation. *Nat. Commun.* **2024**, *15*, 2000.
56. Ahn, H.-Y.; Walters, J.B.; Avila, R.; et al. Bioresorbable, wireless dual stimulator for peripheral nerve regeneration. *Nat. Commun.* **2025**, *16*, 4752.
57. Wang, L.; Zhang, T.; Lei, J.; et al. A biodegradable and restorative peripheral neural interface for the interrogation of neuropathic injuries. *Nat. Commun.* **2025**, *16*, 1716.
58. Huang, I.; Zhang, Y.; Arafa, H.M.; et al. High performance dual-electrolyte magnesium–iodine batteries that can harmlessly resorb in the environment or in the body. *Energy Environ. Sci.* **2022**, *15*, 4095–4108.
59. Lv, Y.; Liu, X.; Liu, J.; et al. Implantable and bio-compatible Na-O2 battery. *Chem* **2024**, *10*, 1885–1896.

60. Lee, D.-M.; Kang, M.; Hyun, I.; et al. An on-demand bioresorbable neurostimulator. *Nat. Commun.* **2023**, *14*, 7315.
61. Hu, Z.; Guo, H.; An, D.; et al. Bioresorbable multilayer organic–inorganic films for bioelectronic systems. *Adv. Mater.* **2024**, *36*, 2309421.
62. Huang, Y.; Li, H.; Hu, T.; et al. Implantable electronic medicine enabled by bioresorbable microneedles for wireless electrotherapy and drug delivery. *Nano Lett.* **2022**, *22*, 5944–5953.
63. Kaveti, R.; Lee, J.H.; Youn, J.K.; et al. Soft, long-lived, bioresorbable electronic surgical mesh with wireless pressure monitor and on-demand drug delivery. *Adv. Mater.* **2024**, *36*, 2307391.
64. Sheng, H.; Jiang, L.; Wang, Q.; et al. A soft implantable energy supply system that integrates wireless charging and biodegradable Zn-ion hybrid supercapacitors. *Sci. Adv.* **2023**, *9*, eadh8083.
65. Muniraj, V.K.A.; Vijayan, B.L.; Hammoud, H.; et al. Bioresorbable and wireless rechargeable implanted Na-ion battery for temporary medical devices. *Adv. Funct. Mater.* **2025**, *35*, 2417353.
66. Fang, Y.; Prominski, A.; Rotenberg, M.Y.; et al. Micelle-enabled self-assembly of porous and monolithic carbon membranes for bioelectronic interfaces. *Nat. Nanotechnol.* **2021**, *16*, 206–213.
67. Singh, N.; Singh, V.; Bisht, N.; et al. A comprehensive review on supercapacitors: Basics to recent advancements. *J. Energy Storage* **2025**, *121*, 116498.
68. Kumar, N.; Lee, S.-Y.; Park, S.-J. Bridging EDLC and pseudocapacitive mechanisms through materials design: Recent advances in supercapacitor electrodes. *Curr. Opin. Solid State Mater. Sci.* **2026**, *41*, 101251.
69. Kumar, N.; Kim, S.-B.; Lee, S.-Y.; et al. Recent advanced supercapacitor: A review of storage mechanisms, electrode materials, modification, and perspectives. *Nanomaterials* **2022**, *12*, 3708.
70. Ansari, S.A.; Parveen, N.; Ansari, M.Z.; et al. Exploring recent advances in the versatility and efficiency of carbon materials for next generation supercapacitor applications: A comprehensive review. *Prog. Mater. Sci.* **2025**, *154*, 101493.
71. Jovanović, P.; Sharifzadeh Mirshekarloo, M.; Aitchison, P.; et al. Operando interlayer expansion of multiscale curved graphene for volumetrically-efficient supercapacitors. *Nat. Commun.* **2025**, *16*, 8271.
72. Chen, G.; Han, F.; Lin, D.; et al. Three-dimensional multi-layer carbon tube electrodes for AC line-filtering capacitors. *Joule* **2024**, *8*, 1080–1091.
73. Na, Y.W.; Cheon, J.Y.; Kim, J.H.; et al. All-in-one flexible supercapacitor with ultrastable performance under extreme load. *Sci. Adv.* **2022**, *8*, eabl8631.
74. Park, H.W.; Roh, K.C. Recent advances in and perspectives on pseudocapacitive materials for Supercapacitors–A review. *J. Power Sources* **2023**, *557*, 232558.
75. Schoetz, T.; Gordon, L.W.; Ivanov, S.; et al. Disentangling faradaic, pseudocapacitive, and capacitive charge storage: A tutorial for the characterization of batteries, supercapacitors, and hybrid systems. *Electrochim. Acta* **2022**, *412*, 140072.
76. Sahoo, S.; Kumar, R.; Joanni, E.; et al. Advances in pseudocapacitive and battery-like electrode materials for high performance supercapacitors. *J. Mater. Chem. A* **2022**, *10*, 13190–13240.
77. Gu, Y.; Zhang, Y.; Wang, X.; et al. Defect engineered nickel hydroxide nanosheets for advanced pseudocapacitor electrodes. *Nano Res.* **2024**, *17*, 5233–5242.
78. Sharma, S.; Kadyan, P.; Sharma, R.K.; et al. Progressive updates on nickel hydroxide and its nanocomposite for electrochemical electrode material in asymmetric supercapacitor device. *J. Energy Storage* **2024**, *87*, 111368.
79. Meng, Y.; Liang, C.; Jiang, D.; et al. Ion modified cobalt-based layered double hydroxides and its derivatives as electrode materials for supercapacitors: A review and perspective. *J. Energy Storage* **2023**, *74*, 109105.
80. Khaleque, Md. A.; Aly Saad Aly, M.; Khan, Md. Z. H. Chemical and electrochemical synthesis of doped conducting polymers and their application in supercapacitors: An overview. *Chem. Eng. J.* **2025**, *507*, 160444.
81. Li, L.; Ai, Z.; Wu, J.; et al. A robust polyaniline hydrogel electrode enables superior rate capability at ultrahigh mass loadings. *Nat. Commun.* **2024**, *15*, 6591.
82. Vipu Vinayak, V.J.; Deshmukh, K.; Murthy, V.R.K.; et al. Conducting polymer based nanocomposites for supercapacitor applications: A review of recent advances, challenges and future prospects. *J. Energy Storage* **2024**, *100*, 113551.
83. Li, C.; Zhang, K.; Cheng, X.; et al. Polymers for flexible energy storage devices. *Prog. Polym. Sci.* **2023**, *143*, 101714.
84. Ahmed, S.; Ahmed, A.; Basha, D.B.; et al. Critical review on recent developments in conducting polymer nanocomposites for supercapacitors. *Synth. Met.* **2023**, *295*, 117326.
85. Reenu; Sonia; Phor, L.; Chahal, S. Electrode materials for supercapacitors: A comprehensive review of advancements and performance. *J. Energy Storage* **2024**, *84*, 110698.
86. Saju, D.M.; Sapna, R.; Deka, U.; et al. MXene material for supercapacitor applications: A comprehensive review on properties, synthesis and machine learning for supercapacitance performance prediction. *J. Power Sources* **2025**, *647*, 237302.
87. Gao, M.; Wang, F.; Yang, S.; et al. Engineered 2D MXene-based materials for advanced supercapacitors and micro-supercapacitors. *Mater. Today* **2024**, *72*, 318–358.
88. Wang, W.; Chen, D.; Li, F.; et al. Metal-organic-framework-based materials as platforms for energy applications. *Chem* **2024**, *10*, 86–133.

89. Zhao, W.; Zeng, Y.; Zhao, Y.; et al. Recent advances in metal-organic framework-based electrode materials for supercapacitors: A review. *J. Energy Storage* **2023**, *62*, 106934.
90. Chaluvachar, P.; Sudhakar, Y.N.; Mahesha, G.T.; et al. Polyoxometalate-based hybrid supercapacitors: Advances, challenges, and future prospects in sustainable energy storage. *Chem. Eng. J. Adv.* **2025**, *24*, 100908.
91. Xin, X.; Xu, Y.; Zhou, M.; et al. Black phosphorus hybrid films enabled by a covalently chemical and spatial hierarchical-locking effect for flexible supercapacitors with 100% cycling stability. *J. Mater. Chem. A* **2024**, *12*, 26083–26095.
92. Kulkarni, A.A.; Gaikwad, N.K.; Bhat, T.S. Black phosphorus: Envisaging the opportunities for supercapacitors. *J. Electroanal. Chem.* **2023**, *942*, 117543.
93. Sim, H.J.; Choi, C.; Lee, D.Y.; et al. Biomolecule based fiber supercapacitor for implantable device. *Nano Energy* **2018**, *47*, 385–392.
94. Xue, Y.; Zhang, Z.; Liu, D.; et al. Advances in electrode and electrolyte materials of fiber-shaped supercapacitors for electrochemical performance improvement and applications extension. *Energy Storage Mater.* **2025**, *77*, 104222.
95. Wang, K.; Wang, Z.; Wang, C.; et al. Carbon fiber electrodes for composite structural supercapacitor: Preparation and modification methods. *J. Energy Storage* **2024**, *98*, 113129.
96. Jeon, S.; Seo, H.; Kim, Y.; et al. Fully biocompatible, thermally drawn fiber supercapacitors for long-term bio-implantation. *Nat. Commun.* **2025**, *16*, 8207.
97. Gao, C.; Liu, J.; Han, Y.; et al. An energy-adjustable, deformable, and packable wireless charging fiber supercapacitor. *Adv. Mater.* **2024**, *36*, 2413292.
98. Wang, S.; Liu, N.; Su, J.; et al. Highly stretchable and self-healable supercapacitor with reduced graphene oxide based fiber springs. *ACS Nano* **2017**, *11*, 2066–2074.
99. Wang, H.; Liu, Z.; Ding, J.; et al. Downsized sheath–core conducting fibers for weavable superelastic wires, biosensors, supercapacitors, and strain sensors. *Adv. Mater.* **2016**, *28*, 4998–5007.
100. Chen, T.; Hao, R.; Peng, H.; et al. High-performance, stretchable, wire-shaped supercapacitors. *Angew. Chem. Int. Ed.* **2015**, *54*, 618–622.
101. Manjakkal, L.; Pullanchiyodan, A.; Yogeswaran, N.; et al. A wearable supercapacitor based on conductive PEDOT:PSS-coated cloth and a sweat electrolyte. *Adv. Mater.* **2020**, *32*, 1907254.
102. Wu, Z.; Parvez, K.; Feng, X.; et al. Graphene-based in-plane micro-supercapacitors with high power and energy densities. *Nat. Commun.* **2013**, *4*, 2487.
103. Kim, H.; Yoon, J.; Lee, G.; et al. Encapsulated, high-performance, stretchable array of stacked planar micro-supercapacitors as waterproof wearable energy storage devices. *ACS Appl. Mater. Interfaces* **2016**, *8*, 16016–16025.
104. Fan, Z.; Liu, Y.; Yan, J.; et al. Template-directed synthesis of pillared-porous carbon nanosheet architectures: High-performance electrode materials for supercapacitors. *Adv. Energy Mater.* **2012**, *2*, 419–424.
105. Gao, C.; Huang, J.; Xiao, Y.; et al. A seamlessly integrated device of micro-supercapacitor and wireless charging with ultrahigh energy density and capacitance. *Nat. Commun.* **2021**, *12*, 2647.
106. Lei, Z.; Liu, L.; Zhao, H.; et al. Nanoelectrode design from microminiaturized honeycomb monolith with ultrathin and stiff nanoscaffold for high-energy micro-supercapacitors. *Nat. Commun.* **2020**, *11*, 299.
107. Robert, K.; Douard, C.; Demortière, A.; et al. On-chip interdigitated micro-supercapacitors based on sputtered bifunctional vanadium nitride thin films with finely tuned inter- and intracolumnar porosities. *Adv. Mater. Technol.* **2018**, *3*, 1800036.
108. Cheng, T.; Zhang, Y.-Z.; Zhang, J.-D.; et al. High-performance free-standing PEDOT:PSS electrodes for flexible and transparent all-solid-state supercapacitors. *J. Mater. Chem. A* **2016**, *4*, 10493–10499.
109. Xu, P.; Kang, J.; Choi, J.-B.; et al. Laminated ultrathin chemical vapor deposition graphene films based stretchable and transparent high-rate supercapacitor. *ACS Nano* **2014**, *8*, 9437–9445.
110. Cao, L.; Wang, C.; Huang, Y. Structure optimization of graphene aerogel-based composites and applications in batteries and supercapacitors. *Chem. Eng. J.* **2023**, *454*, 140094.
111. Gong, X.; Zhang, X.; Wang, D.; et al. Three-dimensional graphene aerogel materials for supercapacitors: Strategies and mechanisms. *Energy Environ. Mater.* **2025**, *8*, e70054.
112. Lin, X.; Sheng, L.; Yang, J.; et al. Flexible films with three-dimensional ion transport channels: Carbon nanotubes@MnO_2 as interlayer spacers in porous graphene electrodes for high-performance supercapacitors. *J. Alloys Compd.* **2024**, *990*, 174455.
113. Ran, J.; Liu, Y.; Feng, H.; et al. A review on graphene-based electrode materials for supercapacitor. *J. Ind. Eng. Chem.* **2024**, *137*, 106–121.
114. Pramoda, K.; Rao, C.N.R. Electrostatic restacking of two-dimensional materials to generate novel hetero-superlattices and their energy applications. *APL Mater.* **2023**, *11*, 020901.
115. Deshmukh, S.; Ghosh, K.; Pykal, M.; et al. Laser-induced MXene-functionalized graphene nanoarchitectonics-based microsupercapacitor for health monitoring application. *ACS Nano* **2023**, *17*, 20537–20550.

116. Wu, Y.; Ma, B.; Cheng, S.; et al. Three-dimensional micro/nano-interconnected scaffold graphene-based micro-supercapacitors with high electrochemical performance. *Electrochim. Acta* **2022**, *427*, 140864.
117. Yan, X.; Zu, K.; Tang, J.; et al. A membrane-less Zn-air biobattery/supercapacitor hybrid device. *J. Energy Storage* **2024**, *88*, 111469.
118. Zhang, Y.; Deng, H.; Zheng, Y.; et al. Pseudocapacitance behavior enables efficient and stable electrochemical energy conversion and storage in glucose/air enzymatic biofuel cells. *J. Energy Storage* **2024**, *82*, 110604.
119. Qian, Z.; Yang, Y.; Wang, L.; et al. An implantable fiber biosupercapacitor with high power density by multi-strand twisting functionalized fibers. *Angew. Chem. Int. Ed.* **2023**, *62*, e202303268.
120. Guan, S.; Yang, Y.; Wang, Y.; et al. A dual-functional MXene-based bioanode for wearable self-charging biosupercapacitors. *Adv. Mater.* **2024**, *36*, 2305854.
121. Han, M.; Srivastava, S.B.; Yildiz, E.; et al. Organic photovoltaic pseudocapacitors for neurostimulation. *ACS Appl. Mater. Interfaces* **2020**, *12*, 42997–43008.
122. Chae, J.S.; Heo, N.-S.; Kwak, C.H.; et al. A biocompatible implant electrode capable of operating in body fluids for energy storage devices. *Nano Energy* **2017**, *34*, 86–92.
123. Chae, J.S.; Lee, H.; Kim, S.H.; et al. A durable high-energy implantable energy storage system with binder-free electrodes useable in body fluids. *J. Mater. Chem. A* **2022**, *10*, 4611–4620.
124. Su, Y.; Li, N.; Wang, L.; et al. Stretchable transparent supercapacitors for wearable and implantable medical devices. *Adv. Mater. Technol.* **2022**, *7*, 2270004.
125. Liu, Y.; Zhou, H.; Zhou, W.; et al. Biocompatible, high-performance, wet-adhesive, stretchable all-hydrogel supercapacitor implant based on PANI@rGO/Mxenes electrode and hydrogel electrolyte. *Adv. Energy Mater.* **2021**, *11*, 2101329.
126. Zeng, X.; Guo, Y.; Wei, X.; et al. A biodegradable and flexible solid-state supercapacitor based on a natural polymer dual network hydrogel electrolyte. *J. Mater. Chem. A* **2025**, *13*, 34938–34947.
127. Wang, E.; Wu, M.; Luo, L.; et al. Symbiotic biodegradable flexible supercapacitor *in vivo*. *Device* **2025**, *3*, 100724.
128. Lee, G.; Kang, S.-K.; Won, S.M.; et al. Fully Biodegradable Microsupercapacitor for Power Storage in Transient Electronics. *Adv. Energy Mater.* **2017**, *7*, 1700157.
129. Mendhe, A.; Panda, H.S. A review on electrolytes for supercapacitor device. *Discov. Mater.* **2023**, *3*, 29.
130. Luo, P.; Liu, Q.; Chen, R.; et al. Recent progress in biocompatible miniature supercapacitors. *Energy Mater.* **2025**, *5*, 500070.
131. Lee, J.; Park, S.; Choi, Y. Organic encapsulants for bioresorbable medical electronics. *MRS Bull.* **2024**, *49*, 247–255.
132. McDonald, S.M.; Yang, Q.; Hsu, Y.-H.; et al. Resorbable barrier polymers for flexible bioelectronics. *Nat. Commun.* **2023**, *14*, 7299.
133. Hwangbo, J.; Seo, H.; Sim, G.; et al. Bioresorbable polymers for electronic medicine. *Cell Rep. Phys. Sci.* **2024**, *5*, 102099.
134. Gao, C.; Bai, C.; Gao, J.; et al. A directly swallowable and ingestible micro-supercapacitor. *J. Mater. Chem. A* **2020**, *8*, 4055–4061.
135. Li, H.; Zhao, C.; Wang, X.; et al. Fully bioabsorbable capacitor as an energy storage unit for implantable medical electronics. *Adv. Sci.* **2019**, *6*, 1801625.
136. Zhao, C.; Park, J.; Root, S.E.; et al. Skin-inspired soft bioelectronic materials, devices and systems. *Nat. Rev. Bioeng.* **2024**, *2*, 671–690.
137. Han, D.; Kim, M.; Lee, S.; et al. A review of yarn-based one-dimensional supercapacitors. *Nanomaterials* **2023**, *13*, 2581.
138. Chen, Y.; Xu, B.; Wen, J.; et al. Design of novel wearable, stretchable, and waterproof cable-type supercapacitors based on high-performance nickel cobalt sulfide-coated etching-annealed yarn electrodes. *Small* **2018**, *14*, 1704373.
139. Shin, D.; Shen, C.; Sanghadasa, M.; et al. Breathable 3D supercapacitors based on activated carbon fiber veil. *Adv. Mater. Technol.* **2018**, *3*, 1800209.
140. Zhu, S.; Li, Y.; Zhu, H.; et al. Pencil-drawing skin-mountable micro-supercapacitors. *Small* **2019**, *15*, 1804037.
141. Luan, P.; Zhang, N.; Zhou, W.; et al. Epidermal supercapacitor with high performance. *Adv. Funct. Mater.* **2016**, *26*, 8178–8184.
142. An, T.; Ling, Y.; Gong, S.; et al. A wearable second skin-like multifunctional supercapacitor with vertical gold nanowires and electrochromic polyaniline. *Adv. Mater. Technol.* **2019**, *4*, 1800473.
143. Gong, S.; Cheng, W. Toward soft skin-like wearable and implantable energy devices. *Adv. Energy Mater.* **2017**, *7*, 1700648.
144. Song, P.; Kuang, S.; Panwar, N.; et al. A self-powered implantable drug-delivery system using biokinetic energy. *Adv. Mater.* **2017**, *29*, 1605668.
145. Kang, S.-K.; Murphy, R.K.J.; Hwang, S.-W.; et al. Bioresorbable silicon electronic sensors for the brain. *Nature* **2016**, *530*, 71–76.
146. Araci, I.E.; Su, B.; Quake, S.R.; et al. An implantable microfluidic device for self-monitoring of intraocular pressure. *Nat. Med.* **2014**, *20*, 1074–1078.
147. Zheng, Q.; Shi, B.; Fan, F.; et al. *In vivo* powering of pacemaker by breathing-driven implanted triboelectric nanogenerator. *Adv. Mater.* **2014**, *26*, 5851–5856.

148. Jang, Y.; Park, T.; Kim, E.; et al. Implantable biosupercapacitor inspired by the cellular redox system. *Angew. Chem. Int. Ed.* **2021**, *60*, 10563–10567.
149. Sheng, H.; Zhou, J.; Li, B.; et al. A thin, deformable, high-performance supercapacitor implant that can be biodegraded and bioabsorbed within an animal body. *Sci. Adv.* **2021**, *7*, eabe3097.
150. Kim, D.-H.; Lu, N.; Ma, R.; et al. Epidermal electronics. *Science* **2011**, *333*, 838–843.
151. Feiner, R.; Dvir, T. Tissue–electronics interfaces: From implantable devices to engineered tissues. *Nat. Rev. Mater.* **2017**, *3*, 17076.
152. Deng, J.; Yuk, H.; Wu, J.; et al. Electrical bioadhesive interface for bioelectronics. *Nat. Mater.* **2021**, *20*, 229–236.
153. Wang, S.; Xu, J.; Wang, W.; et al. Skin electronics from scalable fabrication of an intrinsically stretchable transistor array. *Nature* **2018**, *555*, 83–88.
154. Sheng, X.; Du, Z.; Gao, Z.; et al. An implantable in-hydrogel wireless supercapacitor-activated neuron system enables bidirectional modulation. *Adv. Mater.* **2025**, *37*, 2504558.